

Rcrust: a tool for calculating *path-dependent* open system processes and application to melt loss

by

Matthew Jason Mayne

*Thesis presented in fulfilment of the requirements for the degree of Master of Science in the Faculty of
Science at Stellenbosch University*



Supervisor: Prof. Gary Stevens, Stellenbosch University

Co-supervisor: Prof Jean-François Moyen, Université de Saint-Etienne (France)

March 2016

Declaration

By submitting this thesis electronically, I declare that the entirety of the work contained therein is my own, original work, that I am the sole author thereof (save to the extent explicitly otherwise stated), that reproduction and publication thereof by Stellenbosch University will not infringe any third party rights and that I have not previously in its entirety or in part submitted it for obtaining any qualification.

March 2016

ABSTRACT

Earth's continental crust is stabilised by crustal differentiation that is driven by partial melting and melt loss: Magmas segregate from their residuum and migrate into the upper crust, leaving the deep crust refractory. Thus, compositional change is an integral part of the metamorphic evolution of anatectic granulites. Current thermodynamic modelling techniques have limited abilities to handle changing bulk composition. New software is developed (Rcrust) that via a path-dependent iteration approach enables pressure, temperature and bulk composition to act as simultaneous variables. Path-dependence allows phase additions or extractions that will alter the effective bulk composition of the system. This new methodology leads to a host of additional investigative tools. Singular paths within Pressure-Temperature-Bulk composition (P - T - X) space give details of changing phase proportions and compositions during the anatectic process, while compilations of paths create *path-dependent* P - T mode diagrams. A case study is used to investigate the effects of melt loss in an open system for a pelite starting bulk composition. The study is expanded upon by considering multiple P - T paths and considering the effects of a lower melt threshold. It is found that, for the pelite starting composition under investigation, open systems produce less melt than closed systems and that melt loss prior to decompression drastically reduces the ability of the system to form melt upon decompression.

Keywords: Rcrust, anatexis; melt loss; thermodynamic modelling; decompression melting

OPSOMMING

Korsdifferensiasie stabiliseer die kontinentale kors van die aarde tydens gedeeltelike smelting. Magma segregeer van hul residuum en migreer in die vlakker kors in. As gevolg daarvan raak die diepkors meer vuurvas. Dus speel komposisionele verandering 'n belangrike rol in die evolusie van anatektiese granuliete. Hedendaagse termodinamiese modelleringstegnieke het beperkte vermoëns om 'n veranderende grootmaatsamestelling te hanteer. Nuwe sagteware is ontwikkel (Rcrust) wat 'n roete-afhanklike iterasie benadering volg. Hierdie metode laat die druk, temperatuur en grootmaatsamestelling toe om as gelyktydige veranderlikes te funksioneer. Roete-afhanklikheid laat fase-toevoegings of ekstraksies toe om die effektiewe grootmaatsamestelling van die stelsel te verander. Die nuwe metode bied 'n magdom verskeie maniere aan om ondersoek in te stel. Enkel roetes van P - T - X ruimte beskryf die fase proporsies en komposisies tydens die proses anatektiese, terwyl kombinasies van roetes, roete-afhanklike pseudoseksies skep. 'n Gevallestudie is op uitgebrei om die gevolge van smeltverlies te ondersoek. Dit is bevind dat oop stelsels minder produktief by smelt vorming is as geslote stelsels, en dat dekompressie smelt minder produktief as verwarming is. Die verlies in smelt produktiwiteit van die oop stelsel impliseer beperkings op die maksimum massa dekompressie smelt wat kan vorm. Tektoniese modelle wat dekompressie smelt as bron van groot volumes smelt gebruik moet dus herevalueer word.

Sleutelwoorde: Rcrust, Anatekse, smeltverlies, termodinamiese modellering, dekompressie smelt

ACKNOWLEDGEMENTS

Funding by the South African National Research Foundation (NRF) through the Scare Skills Bursary to M.J. Mayne and from the South African Research Chairs Initiative (SARChI) to G. Stevens is gratefully acknowledged. M.J. Mayne would like to acknowledge support from the European Research Council (project MASE, ERC StG 279828 to J. van Hunen).

I would like to thank my supervisors Prof. Gary Stevens and Prof. Jeff Moye for their constant attention and assistance throughout the project. In addition, I would like to thank my family and friends for their support and patience. This work was orally presented by M.J. Mayne at the Granulites & granulites conference, 2015 in Windhoek, Namibia.

TABLE OF CONTENTS

	Page
Declaration	ii
Abstract	iii
Opsomming	iv
Acknowledgements	v
Table of Contents	vi
List of Figures	viii
List of Tables	x
List of Abbreviations	xi
Chapter 1: Contributions of the authors	1
Chapter 2: Presentation of the Research Paper: Rcrust: a tool for calculating <i>path-dependent</i> open system processes and application to melt loss	2
Abstract	4
1. Introduction	5
1.1. Thermodynamic modelling tools	5
1.3. Modelling compositional change in <i>P-T-X</i> space	6
2. Rcrust: A <i>Path-Dependent</i> Approach	7
2.1. How it works	9
2.2. Custom functions - magma extraction	10
2.3. Outputs	11
3. Program Description	11

3.1. Thermodynamic calculations	11
3.2. Code manipulations	12
3.3. User interface	12
4. Case Study	13
4.1. Model set up by Yakymchuck & Brown (2014)	13
4.2. Reproducing the results	15
4.3. Comparing the results	16
4.4. Clocksie P - T path	17
4.5. Multi-path functionality	19
4.6. Exploring new functionality	19
5. Results – Effects of Melt loss	21
5.1. Isobaric heating (IBH)	21
5.2. Isothermal decompression (ITD)	22
5.3. Melt crystallisation zones	25
5.3 Lower melt threshold investigation	27
5.5. Melt productivity	30
6. Discussion	32
6.1. Effects of melt loss	32
6.2. Rcrust	33
7. Conclusion	34
Acknowledgements	35
References	36
Supplementary Figures	43

Chapter 3: Addenda

LIST OF FIGURES

		Page
Fig. 1	Flow chart of the Rcrust program structure	8
Fig. 2	Drop down based Rcrust GUI	10
Fig. 3	Flow chart of the magma extraction algorithm	11
Fig. 4	Rcrust P - T psuedosection with phase proportion paths for the isobaric heating path at 12 kbar (IBH12)	15
Fig. 5	Rcrust clockwise P - T path and phase mode diagrams	18
Fig. 6	Contour plots of biotite, muscovite and total melt in the full system for the closed system case as well as <i>path-dependent</i> P - T mode diagram for a compilation of isobaric heating paths	20
Fig. 7	Contour plots for 7 vol.% threshold <i>path-dependent</i> P - T mode diagrams showing interstitial melt, total melt and H ₂ O in the residuum for the isobaric heating system and the 12kbar isobaric heating followed by isothermal decompression system	24
Fig. 8	Phase boundaries and garnet-biotite mode difference for the 7 vol.% threshold 12kbar isobaric heating followed by isothermal decompression system	26
Fig. 9	Contour plots for 1 vol.% threshold <i>path-dependent</i> P - T mode diagrams showing interstitial melt, total melt and H ₂ O in the residuum for the isobaric heating system and the 12kbar isobaric heating followed by isothermal decompression system	29

	Page
Fig. 10 Melt productivity difference (MPD) contours for 1 vol.% threshold <i>path-dependent P-T</i> mode diagrams	31

SUPPLEMENTARY FIGURES

Sup Fig. 1 Contour plots for <i>P-T</i> modes in the closed system	43
Sup Fig. 2 Contour plots for <i>path-dependent P-T</i> modes in the 7 vol.% threshold isobaric heating system	44
Sup Fig. 3 Contour plots for <i>path-dependent P-T</i> modes in the 7 vol.% threshold 12kbar isobaric heating followed by isothermal decompression system	45
Sup Fig. 4 Contour plots for <i>path-dependent P-T</i> modes in the 1 vol.% threshold isobaric heating system	46
Sup Fig. 5 Contour plots for <i>path-dependent P-T</i> modes in the 1 vol.% threshold 12kbar isobaric heating followed by isothermal decompression system	47

LIST OF TABLES

	Page
Table 1 Starting bulk composition used in the construction of pseudosections	14

LIST OF ABBREVIATIONS

Minerals:

Abbreviations for rock forming minerals were taken from Whitney & Evans (2010) as:

And	Andalusite
Bt	Biotite
Cpx	Clinopyroxene
Crd	Cordierite
Grt	Garnet
H ₂ O	Water
Ilm	Ilmenite
Kfs	Alkali feldspar
Ky	Kyanite
Liq	Liquid
Mag	Magnetite
Ms	Muscovite
Opx	Orthopyroxene
Pl	Plagioclase feldspar
Qz	Quartz
Sil	Sillimanite
Spl	Spinel

Terminology:

AS	Addition subsystem
ES	Extract subsystem
FS	Full system
ΔG	Change in Gibbs free energy of the system
GUI	Graphical user interface
IBH	Isobaric heating
IBH12	Isobaric heating at 12 kbar pressure
ITD	Isothermal decompression
MCT	Melt Connectivity Transition
ML	Melt loss event
mol.%	molar percentage
mol*,%	one oxide normalised molar percentage
NCKFMASHTO	$\text{Na}_2\text{O}-\text{CaO}-\text{K}_2\text{O}-\text{FeO}-\text{MgO}-\text{Al}_2\text{O}_3-\text{SiO}_2-\text{H}_2\text{O}-\text{TiO}_2-\text{O}$
PAE	Peritectic assemblage entrainment
<i>P-T-X</i>	Pressure-Temperature-Bulk composition
RS	Reactive subsystem
TCL	Tool Command Language
vol.%	volume percentage
wt.%	weight percentage

CHAPTER 1

CONTRIBUTIONS OF THE AUTHORS

Professor Jean-François Moyen along with Professor Vojtěch Janoušek created the first form of Rcrust using a phase stability calculation routine that called meemum from the Perple_X suite of programs as an executable. I was introduced to the program and the R coding language by Professor Moyen after which I took over further development of Rcrust.

I wrote a new phase stability calculation routine which uses a wrapper (compiled by Dr Lars Kaislaniemi) to perform calculations directly in the global environment making it quicker and more robust. I created save and load routines whereby simulation parameters are communicated through a text document. I developed initialisation routines for starting variables and severed the need for an initial meemum build file. I then created a graphical user interface to allow ease of use. I introduced the idea of a full system which is split into addition; extraction and reactive subsystems with routines that pass phases between them. I created some rudimentary output routines including a colour map using identification numbers of unique phase assemblages encountered by points along a path.

To investigate the uses of Rcrust, I performed a case study which reproduced the results of Yakymchuk & Brown (2014) but without using the manual stitching together of pseudosections. I expanded this case study by compiling *P-T-X* paths into a new type of diagram we call *path-dependent P-T* mode diagrams which I used to investigate the effects of melt loss on the total melt productivity of open systems (Chapter 2: Presentation of the research paper). I then developed these results into a manuscript which was submitted to the Journal of Metamorphic Geology. Throughout the coding and writing processes Professor Gary Stevens and Professor Jean-François Moyen provided academic guidance. Dr Lars Kaislaniemi compiled the Perple_X wrapper and provided insightful comments on the final manuscript.

REFERENCES

Yakymchuk, C. & Brown, M., 2014. Consequences of open-system melting in tectonics. *Journal of the Geological Society*, **171**, 21-40.

CHAPTER 2

PRESENTATION OF THE RESEARCH PAPER

Rcrust: a tool for calculating *path-dependent* open system processes and application to melt loss

M. J. MAYNE^{1,2,*}, J.-F. MOYEN², G. STEVENS¹, L. KAISLANIEMI³

1 Center for Crustal Petrology, Department of Earth Sciences, Stellenbosch University,
Private Bag X1, Matieland 7602, South Africa

2 Université Jean Monnet, 23 Rue du Docteur Paul Michelin, 42023 Saint-Etienne, Cedex 2,
France

3 Institute of Seismology, Department of Geosciences and Geography, University of
Helsinki. Gustaf Hällströmin katu 2b, 00014 Helsinki, Finland

* corresponding author (mmayne@sun.ac.za)

Short title: RCRUST: PATH-DEPENDENT OPEN SYSTEM PROCESSES

ABSTRACT

Earth's continental crust is stabilised by crustal differentiation that is driven by partial melting and melt loss: Magmas segregate from their residuum and migrate into the upper crust, leaving the deep crust refractory. Thus, compositional change is an integral part of the metamorphic evolution of anatectic granulites. Current thermodynamic modelling techniques have limited abilities to handle changing bulk composition. New software is developed (Rcrust) that via a *path-dependent* iteration approach enables pressure, temperature and bulk composition to act as simultaneous variables. *Path-dependence* allows phase additions or extractions that will alter the effective bulk composition of the system. This new methodology leads to a host of additional investigative tools. Singular paths within Pressure-Temperature-Bulk composition (*P-T-X*) space give details of changing phase proportions and compositions during the anatectic process, while compilations of paths create *path-dependent P-T* mode diagrams. A case study is used to investigate the effects of melt loss in an open system for a pelite starting bulk composition. The study is expanded upon by considering multiple *P-T* paths and considering the effects of a lower melt threshold. It is found that, for the pelite starting composition under investigation, open systems produce less melt than closed systems and that melt loss prior to decompression drastically reduces the ability of the system to form melt upon decompression.

Keywords: Rcrust, anatexis; melt loss; thermodynamic modelling; decompression melting

1. INTRODUCTION

Crustal differentiation occurs by partial melting of deep crust at high temperatures (Clemens, 1984; Scaillet *et al.*, 1998), segregation of an incompatible element enriched magma from a more refractory residuum (Clemens & Stevens, 2012) and the migration of the magma to a higher crustal level (Clemens, 1990). Magmas may entrain crystals from the source (Stevens *et al.*, 2007; Villaros *et al.*, 2009; Taylor & Stevens, 2010) and may further evolve through segregation of crystals from melt as the magma ascends and cools (Johnson *et al.*, 2015; Morfin *et al.*, 2014; Sawyer, 2001; Sawyer, 1996). Throughout these processes bulk compositional change of the source and magma is fundamental to crustal differentiation.

Effective bulk composition of the source and of the magma can change throughout the anatexis process by multiple mechanisms. Magma segregation separates the bulk composition into portions that may evolve separately. Varying proportions of peritectic assemblage entrainment (PAE) to the magma influences the bulk compositions of the separated portions (Stevens *et al.*, 2007; Clemens & Stevens, 2012). Kinetic effects can limit the availability of a phase to the system, for example, the slow diffusion of species in plagioclase (Morse, 1984) or garnet (Zuluaga *et al.*, 2005; Taylor & Stevens, 2010) forcing dissolution to be the rate limiting factor or alternatively entire portions of phases can be isolated from reactions by their inclusion in other phases. Thus the effective bulk composition of the system is dependent on the P - T path. Compositional changes of magma and residuum have important implications for further melt production. A recent paper by Yakymchuk & Brown (2014) has criticised the inference of large amounts of decompression melt production across hydrate breakdown reactions. They argued that compositional changes invoked by melt loss on prograde segments of clockwise P - T paths would reduce the ability of the rock to form melt upon suprasolidus decompression. They suggested that large melt volumes, rather than being the result of decompression melting, could be the result of suprasolidus melt transfer and accumulation at shallow levels. Consequently it is crucial for studies of the partial melting of the crust to investigate the combination of pressure (P), temperature (T) and bulk compositional (X) effects.

1.1. Thermodynamic modelling tools

Phase equilibria modelling has contributed enormously to our understanding of the process of anatexis in crustal rocks (White & Powell, 2002; Johnson *et al.*, 2008; White *et al.*, 2007).

Phase equilibria were originally displayed on petrogenetic grids (Albee, 1965). Compositionally relevant phase diagrams were created from these grids by considering a single bulk composition thereby creating pseudosections of P - T - X space (Hensen & Essene, 1971; Hensen & Harley, 1990). The compilation of internally consistent thermodynamic datasets allowed the quantitative calculation of subsolidus phase equilibria (Helgeson *et al.*, 1978; Powell & Holland, 1985; Powell & Holland, 1988; Gottschalk, 1997; Holland & Powell, 1998). Computer programs have been used to create pseudosections by either using the simultaneous solution of non-linear equations as is the case in THERMOCALC (Powell & Holland, 1988; Powell *et al.*, 1998) or the minimisation of Gibbs free energy of the system (ΔG) as is the case in Perple_X (Connolly & Kerrick, 1987) and Theriak/Domino (de Capitani & Petrakakis, 2010). Increased usage of pseudosections in metamorphic studies created a demand for more accurate and applicable solution models which have become more sophisticated with time. The development of solution models for melt (Berman & Brown, 1984; Ghiorso & Sack, 1995; Holland & Powell, 2001; White *et al.*, 2001) allowed thermodynamic modelling to begin to consider partial melting processes.

The behaviour of natural anatectic systems mandates investigations to consider a changing bulk composition. Current software manages a changing bulk composition by setting pressure or temperature constant then scaling between two end members via T - X or P - X sections. This is achieved by using the fractionation abilities of Perple_X or Theriak/Domino (Connolly, 2005; de Capitani & Petrakakis, 2010); by using the 'read bulk info' script from THERMOCALC (Powell *et al.*, 1998) or by manually 'stitching together' different pseudosections each time the bulk composition changes (White & Powell, 2002; Brown & Korhonen, 2009; Yakymchuck & Brown, 2014).

1.2 Modelling compositional change in P - T - X space

Examples of studies investigating compositional change include: water content (e.g. White & Powell, 2002; Johnson *et al.*, 2003; Diener *et al.*, 2008; Johnson *et al.*, 2010; White & Powell, 2010), amount of melt lost from the system (e.g. White & Powell, 2002; Johnson *et al.*, 2003; Johnson *et al.*, 2008; Brown & Korhonen, 2009; Korhonen *et al.*, 2010) or molar proportion of an elemental oxide (e.g. Johnson *et al.*, 2008; Johnson *et al.*, 2010).

Diagrams that require bulk compositional change beyond the capabilities of a binary compositional range are generally created as stitched panels where each panel is a separately calculated pseudosection. An example of this is X scaled as melt loss with separate

panels for each melt loss event (e.g. White & Powell, 2002; Brown & Korhonen, 2009). Phase proportions can be investigated with T - X or P - X diagrams where X is the proportion of the phases (e.g. Johnson & Brown, 2011; Johnson *et al.*, 2010; Johnson *et al.*, 2008; de Capitani & Petrakakis, 2010; White & Powell, 2010; Yakymchuck & Brown, 2014). Advances in software have allowed pressure to vary within a T - X diagram or temperature to vary within a P - X diagram by allowing the user to make one variable dependent on the other thus simulating a P - T path (Connolly, 2005; de Capitani & Petrakakis, 2010).

Graphing compositional change by manually stitching panels becomes prohibitively time consuming when investigating multiple melt loss events or when investigating a variety of bulk compositional controls. This limits the resolution of studies that consider bulk compositional change. The aim of this paper is to introduce a new phase equilibrium modelling tool where pressure, temperature and bulk composition can change simultaneously with an automated handling of bulk compositional change. This paper presents the program's functionalities and the petrological constraints that it operates within. Explanations relating to the code are kept to a minimum with any important coding variables presented in *italics*. A case study is performed to demonstrate the capabilities of the program and highlight the ways in which it can provide added functionality in the study of anatectic systems.

2. RCRUST: A *PATH-DEPENDENT* APPROACH

In this study new software has been developed to provide a functional and efficient tool for investigating crustal anatexis. The software is named 'Rcrust' to emphasise its applicability to crustal anatectic simulations and identify R (Ihaka & Gentleman, 1996) as its coding language. Rcrust operates by calculating the stable phases for a number of points in P - T - X space. For each starting bulk composition chosen a user defined P - T path can be explored.

At each point along this path Rcrust defines the full system (FS) that consists of a reactive subsystem (RS) which is in chemical equilibrium with the P - T - X conditions of the point, an extract subsystem (ES) where phase extractions are stored and an addition subsystem (AS) where phases not yet incorporated in the reactive system are stored (Fig. 1). The extract and addition subsystems are not necessarily in chemical equilibrium with each other, the reactive subsystem or the given P - T - X conditions of the point. Phase extractions and additions, can be performed on the reactive subsystem at set points on the path or

triggered by set criteria met by the reactive subsystem (for example phase abundances in the reactive subsystem can be used to trigger events when a melt threshold is exceeded).

These manipulations (additions or extractions) alter the bulk composition of the reactive subsystem. The final composition of the reactive subsystem at the end of each point's phase manipulations is used as the starting composition of the next point on the path. Points along a path are considered sequentially therefore criteria met in the beginning of a path determine the conditions met by points later in the path. Thus, each point in the P - T - X path calculated is *path-dependent*. Any number of phase manipulations can occur at each P - T - X point allowing pressure, temperature and all n compositional variables of the bulk composition in an n -component system to vary simultaneously. The resolution (number of points) can be increased to make the P - T - X change between each point small enough that a continuous process is effectively mapped.

Stable phases are calculated by calling a compiled form of the *meemum* function from the *Perple_X* suite of programs (Connolly & Kerrick, 1987; Connolly, 2005; Connolly, 2009). This function, given the pressure, temperature and bulk composition of the system, will return the stable mineral phases and their compositions via Gibb's free energy minimisation of the system (ΔG) (Connolly & Kerrick, 1987; Connolly, 2005; Connolly, 2009). The P - T - X conditions for each point in *Rcrust* are passed through the function and the outputs are recorded. Bulk compositional manipulations are performed in *Rcrust* by a series of functions as defined below. The modular form of the functions allows them to be added or changed without affecting the integrity of the overall program.

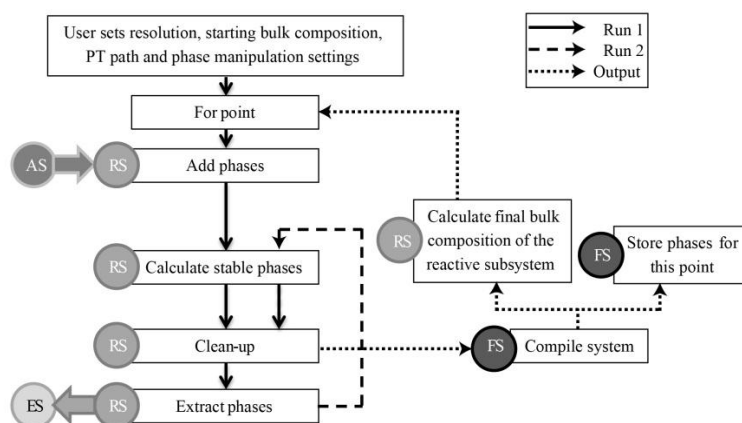


Fig. 1 - Flow chart illustrating the *Rcrust* program structure for a single simple path. The user inputs the calculation's resolution, starting bulk composition, P - T path and phase manipulation settings. Each step in a simulation consists of two runs and an output. The first run is shown in a solid line, the second run in a dashed line and the outputs in a dotted line. Grey circles show the system or subsystem involved in each step as AS (addition subsystem), ES (extract subsystem), FS (full system) or RS (reactive subsystem). Arrows show interactions between systems.

2.1 How it works

The user inputs parameters into an interactive Graphical User Interface (GUI) including initial bulk compositions, P - T paths, thermodynamic dataset, solution models and phase manipulation settings (Fig. 2). The current GUI only has basic functions but will be expanded with future development. P - T paths can be defined by individual points or by a series of functions, allowing consideration of complex P - T paths.

For the first calculable point the starting bulk composition is initialised as the reactive subsystem and used to calculate the stable phases under the given P - T - X conditions. If no phase manipulations are required at that point then the stable phases will be cleaned up and compiled into a system which records each point's phase compositions, proportions and additional properties. The clean-up process uses abundance and density values from the phase stability calculation to determine the mass and volume of phases. In addition phases' names, that are duplicated due to the presence of solvi in particular solution models (e.g. spinel, feldspar, etc.), are numbered for ease of identification. For convenience any feldspar with more K_2O than CaO (in wt.%) is labelled as "Kf".

Points can undergo phase manipulations consisting of 'phase additions' - phases that are added into the reactive subsystem and 'phase extractions' - phases that are removed from the reactive subsystem. Phase additions are incorporated into the reactive subsystem in the first run of a point so that criteria set on the system take into account the new phase additions (Fig. 1 solid line). Phase extractions operate on the second run of a point so that newly re-equilibrated phase additions can form part of the (extractable) reactive subsystem (Fig. 1 dashed line).

Phase additions and extractions can be invoked at predefined points in the P - T path (*by point*) or when set criteria in the system are met (*by condition*). These conditions can involve any composition, proportion or property of the stable phases. For example, extraction can be set to occur whenever a specified value is exceeded (threshold), such as melt extraction occurring whenever a specified melt proportion is exceeded. Conditions on phase proportions can be given as a weight (wt.%), molar (mol.%) or volume (vol.%) percentages. When phase addition or extraction events are triggered the operations are performed on a mass basis. Alternatively phase extractions can extract a percentage value of the phase present. Outputs from the end of the second run are cleaned up and stored with letters indicating the subsystem it forms part of as either addition subsystem (AS), extract subsystem (ES) or reactive subsystem (RS). Runs are performed sequentially and outputs recorded for the number of points specified by the user.

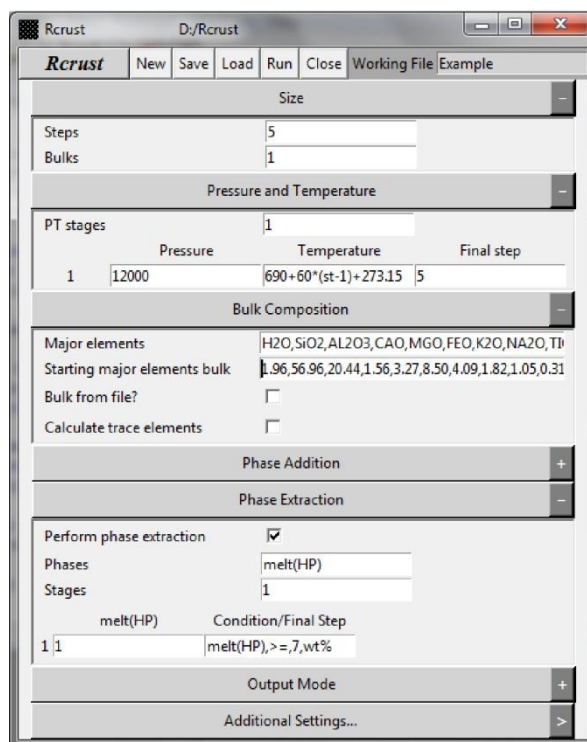


Fig. 2 - Drop down based Rcrust GUI created using the cross-platform (Tcl/Tk) widget toolkit from Ousterhout (1993).

2.2. Custom functions - magma extraction

Phase manipulations can be utilised in their generic forms or customised to suit a petrological problem. For example, as magma extraction from the source is a key aspect of crustal differentiation a custom phase extraction function was set up to model this process (Fig. 3).

The *Extract Magma* function has the same ability to extract *by condition* or *by point* as the standard phase extraction function. The *by condition* argument allows magma extraction to occur whenever a melt threshold is met (the point at which this happens does not need to be known before extraction). Natural magma extraction may leave behind a small amount of melt on grain boundaries (Sawyer, 2001; Marchildon & Brown, 2002; Holness & Sawyer, 2008). Accordingly *Retention mode* enables melt extraction until a set proportion of melt is left (this approximates the melt retention amount). In this study the *Extract Magma* function is used only to extract melt but future studies could consider extracting melt along with crystals (this functionality is currently available in Rcrust). This could be useful to investigate, for example, the entrainment of peritectic phases in a magma.

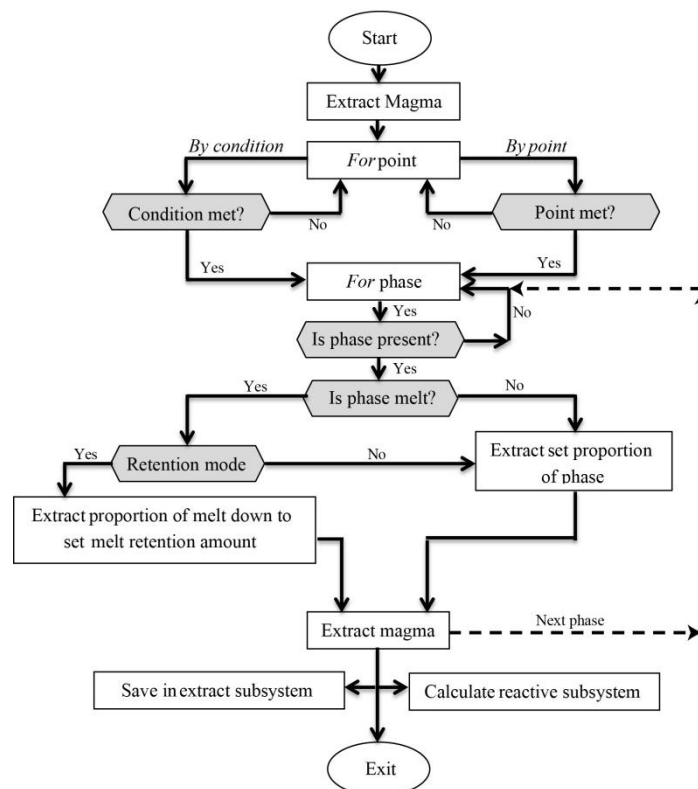


Fig. 3 - Flow chart of the magma extraction algorithm. Grey hexagon shaped boxes are decision points. Coding variables are in *italics*. The *For* phase loop (dotted line) is repeated until each phase tagged for extraction has been considered. If 'Retention mode' is active melt is considered last so that other phases extracted are accounted for in its calculation.

2.3. Outputs

Data from Rcrust can be analysed directly in R, written to file (in text format) or accessed by any R compatible package. One such package, only available for Microsoft Windows®, is Geochemical Data Toolkit (GCDkit). GCDkit is a free package in R that allows plotting of graphical outputs and enables users without a programming knowledge to utilise R's statistical functions (Janoušek *et al.*, 2006).

3. PROGRAM DESCRIPTION

3.1. Thermodynamic calculations

Thermodynamic calculations are performed by a compiled form of the *meemum* function from the Perple_X suite of programs (Connolly & Kerrick, 1987; Connolly, 2005; Connolly,

2009). This is freely available allowing the inclusion of the necessary components in Rcrust's program files, which ensures compatibility across versions and sets the installation options which could otherwise be a source of user error.

3.2. Code manipulations

The program's code is written in R version 2.13.2 (2011-09-30) of R. Copyright © 2011 the R Foundation for Statistical Computing. R is an object-oriented statistical language built to combine the strengths of two other languages: S by Becker *et al.* (1988); and Scheme by Steele & Sussman (1975). This software is open-sourced and requires a machine with at least 32-bit addresses and 2 or more megabytes of directly accessible memory (Ihaka & Gentleman, 1996). R functions on a variety of UNIX platforms, Windows and MacOS.

Calculations in R require no fixed data structures, allow missing values (as 'not applicable' or 'not a number' replies) and follow powerful high level structures. Included in R are multiple arithmetic, statistical and database functions. A limitation of R is that data is stored internally; therefore a system crash results in the loss of the current environment (Ihaka & Gentleman, 1996). Further problems arise in R's complex syntax and non-user-friendly console. The geologist's psychological barrier to programming and the steep learning curve to new programming languages suggest that for a modelling tool to be applied successfully to address problems in the geosciences, it must minimise the interaction between the user and the underlying code. For this purpose a Graphical User Interface (GUI) was constructed.

3.3. User interface

Tool Command Language (TCL) is an embedded command language created by Ousterhout (1993). This language enables a cross-platform widget toolkit (Tcl/Tk) that provides a number of widgets needed to build GUIs. The Tcl/Tk package version 2.13.2 was chosen for the development of the Rcrust GUI for its cross platform capabilities and free format. The current version of the Rcrust GUI however is only stable in the Windows environment. The Tcl/Tk package is included within the Rcrust install files so does not require separate installation from the user. Further, this ensures compatibility between the version of package in which the GUI is both written and displayed.

4. CASE STUDY

In order to assess the validity of Rcrust's calculation routines and the applicability of the program to geological scenarios a case study is performed based on a recent paper ("Consequences of open-system melting in tectonics") by Yakymchuck & Brown (2014). This paper was chosen as it highlights the use of 'pseudosection stitching' to model open system processes.

4.1. Model set up by Yakymchuck & Brown (2014)

Yakymchuck & Brown (2014) used a series of *P-T* pseudosections for bulk chemical compositions modified by a sequence of melt loss events to investigate open-system melting behaviour. The system was set to be conditionally open by extracting melt from the system whenever a melt threshold was exceeded. They modelled two bulk compositions, but for reasons of space here we only investigate the average amphibolite-facies pelite composition that they considered from Ague (1991) (Table 1). Their calculations were performed in THERMOCALC version 3.35 (Powell & Holland, 1988) using the internally consistent dataset of Holland & Powell (1998) in the NCKFMASHTO (Na₂O-CaO-K₂O-FeO-MgO-Al₂O₃-SiO₂-H₂O-TiO₂-O) chemical system. The activity-composition (*a-x*) models they used are stated in Yakymchuck & Brown (2014).

They set the H₂O content of the bulk composition to allow the system to be fully hydrated but with only a small proportion of free fluid (<0.1 mol*.% free H₂O; phase proportions calculated with THERMOCALC output mol.% normalised to a one oxide basis so are referred to in this paper as mol*.) just below the solidus (at 12 kbar). This was done to ensure fluid-absent melting conditions. These normalised mol*.% values approximate volume proportions.

Yakymchuck & Brown (2014) defined melt loss in the open system to occur when an interconnected melt network forms and the matrix compacts. This was considered to happen when >80% of grain boundaries become melt bearing at the rheological transition defined by the Melt Connectivity Transition (MCT) of 7 vol.% melt, the upper limit of the accumulation of melt before extraction (Rosenberg & Handy, 2005). Melt retention on grain boundaries was estimated to be 1 vol.% (Yakymchuck & Brown, 2014). They assumed both of these vol.% constraints to be approximated by equivalent one oxide normalised mol*.%.

Calculations were performed in a P - T area from 2-12 kbar and 640-920 °C (Fig. 4a). In the closed system the biotite stability field extends from 2 to 12 kbar and 640 to 840 °C (Fig. 6a). Muscovite is stable at low temperatures (< 800 °C) and high pressures (> 3 kbar) (Fig. 6b). *Muscovite melting* occurs at pressures above 3 kbar at low temperatures forming a maximum of around 10 wt.% melt at 12 kbar (by using the phrase *muscovite melting* we imply the incongruent melting reaction which consumes muscovite, plagioclase and quartz; similarly by *biotite melting* we imply the incongruent melting reaction which consumes biotite, plagioclase and quartz). Volumetrically the dominant melt producing reaction is that of *biotite melting* at high temperatures and low pressures, producing more than 30 wt.% melt in low pressure regions (Fig. 6c).

The study of Yakymchuck & Brown (2014) approximated simple clockwise P - T paths by first considering an isobaric heating path at 12 kbar (IBH12) followed by isothermal decompression paths at 750 °C (ITD750), 820 °C (ITD820) and 890 °C (ITD890) respectively (Fig. 4a). Each P - T path was investigated as a closed (without melt loss) system and an open (with melt loss) system. To model open system behaviour they manually stitched together pseudosection panels each time melt extraction events occurred (Fig. 4b). Their results suggested that melt extraction on the prograde path reduces residuum fertility thereby impeding the rocks ability to produce large volumes of melt during decompression or further isobaric heating.

Table 1 - Starting bulk composition used in the construction of pseudosections and *path-dependent* P - T mode diagrams in mol.% and wt.% from Yakymchuck & Brown (2014) as the average amphibolite-facies pelite from Ague (1991) after H₂O adjustment to ensure minimal (<0.1 mol*%) free H₂O at the solidus at 12 kbar.

	H ₂ O	SiO ₂	Al ₂ O ₃	CaO	MgO	FeO	K ₂ O	Na ₂ O	TiO ₂	O
mol.%	6.85	59.62	12.61	1.75	5.11	7.44	2.73	1.85	0.83	1.23
wt.%	1.96	56.97	20.45	1.56	3.28	8.50	4.09	1.82	1.05	0.31

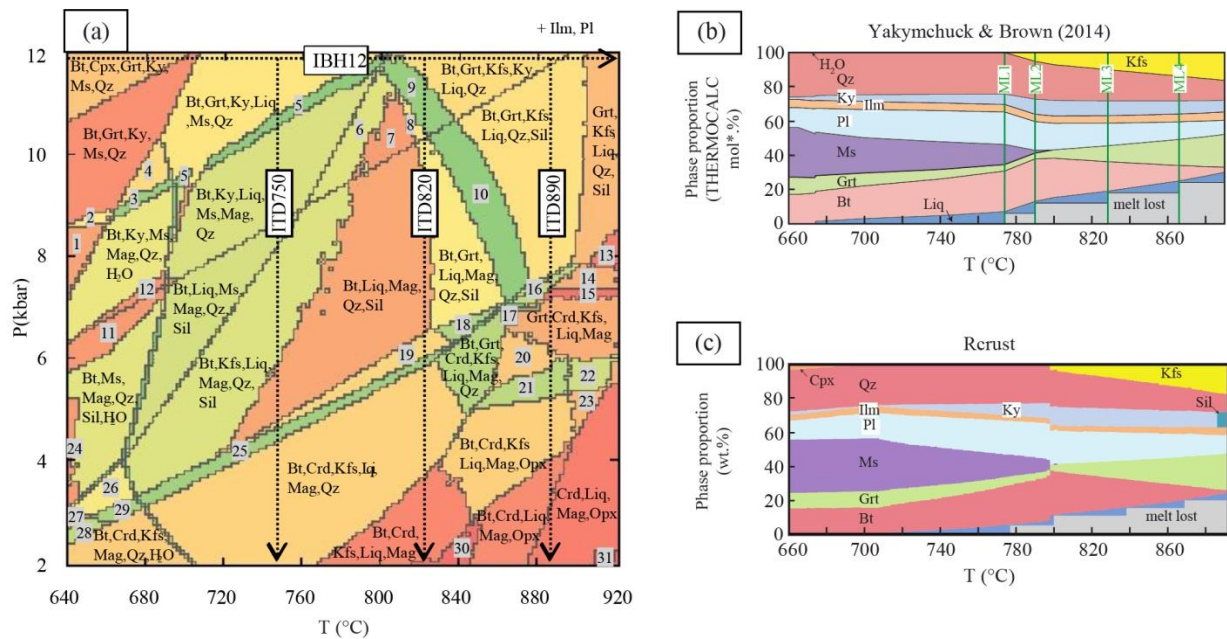


Fig. 4 - (a) Rcrust calculated NCKFMASHTO P - T pseudosection for the bulk composition in Table 1 with arrows showing the P - T paths investigated by Yakymchuck & Brown (2014). (b) From Yakymchuck & Brown (2014) THERMOCALC one oxide normalised molar percentage of phases versus temperature for the path IBH12. (c) Rcrust calculated weight percentage of phases versus temperature for the path IBH12.

IBH = Isobaric heating, ITD = Isothermal decompression, ML = melt loss event. Abbreviations for rock forming minerals were taken from Whitney & Evans (2010) as: And = andalusite, Bt = biotite, Cpx = clinopyroxene, Crd = cordierite, Grt = garnet, H₂O = water, Ilm = ilmenite, Kfs = alkali-feldspar, Ky = kyanite, Liq = liquid, Mag = magnetite, Ms = muscovite, Opx = orthopyroxene, Pl = plagioclase feldspar, Qz = quartz, Sil = sillimanite, Spl = Spinel. Phase assemblages are as follows in addition to Pl and Ilm: 1-Bt,Ky,Ms,Mag,Qz, 2-Bt,Grt,Ky,Ms,Mag,Qz, 3-Bt,Grt,Ky,Ms,Mag,Qz,H₂O, 4-Bt,Grt,Ky,Ms,Qz,H₂O, 5-Bt,Grt,Ky,Liq,Ms,Mag,Qz, 6-Bt,Kfs,Ky,Liq,Mag,Qz, 7-Bt,Ky,Liq,Mag,Qz, 8-Bt,Grt,Ky,Liq,Mag,Qz, 9-Bt,Grt,Kfs,Ky,Liq,Mag,Qz, 10-Bt,Grt,Kfs,Liq,Mag,Qz,Sil, 11-Bt,Kfs,Mag,Qz,Sil,H₂O, 12-Bt,Ky,Ms,Qz,H₂O, 13-Grt,Kfs,Liq,Sil, 14-Grt,Crd,Kfs,Liq,Sil, 15-Grt,Crd,Kfs,Liq, 16-Grt,Crd,Kfs,Liq,Qz,Sil, 17-Grt,Crd,Kfs,Liq,Mag,Qz, 18-Bt,Grt,Crd,Liq,Mag,Qz,Sil, 19-Bt,Crd,Liq,Mag,Qz,Sil, 20-Bt,Grt,Crd,Kfs,Liq,Mag, 21-Bt,Grt,Crd,Kfs,Liq,Mag,Opx, 22-Grt,Crd,Kfs,Liq,Mag,Opx, 23-Crd,Kfs,Liq,Mag,Opx, 24-Bt,Ms,Qz,Sil,H₂O, 25-Bt,Crd,Kfs,Liq,Mag,Qz,Sil, 26-Bt,Kfs,Mag,Qz,Sil,H₂O, 27-And,Bt,Kfs,Mag,Qz,H₂O, 28-And,Bt,Crd,Kfs,Mag,Qz,H₂O, 29-Bt,Crd,Kfs,Mag,Qz,Sil,H₂O, 30-Bt,Crd,Liq,Mag, 31-Crd,Liq,Mag.

4.2. Reproducing the results of Yakymchuck & Brown (2014)

As a proof of concept study and to check the validity of Rcrust's calculations, the paths investigated by Yakymchuck & Brown (2014) were reinvestigated using Rcrust. The H₂O adjusted bulk chemical composition from Yakymchuck & Brown (2014) (Table 1) was used

in the same NCKFMASHTO chemical system. The 2004 revised *hp04ver.dat* thermodynamic file was used with the internally consistent dataset of Holland & Powell (1998). Solution models were chosen which are consistent with the slightly simplified chemistry of the bulk system (e.g. the chemical system does not account for manganese) yet take into account substitutions that are important in stabilising phases (e.g. titanium in biotite). The following solution models were used: feldspar for plagioclase and alkali-feldspars (Fuhrman & Lindsley, 1988; Holland & Powell, 2003), Bio(TCC) for biotite (Tajcmanová *et al.*, 2009), Mica(CHA) for other micas (Coggon & Holland, 2002; Auzanneau *et al.*, 2010), hCrd for cordierite (Holland & Powell, 1998), Gt for garnet (WPH) (White *et al.*, 2007), Opx(HP) for orthopyroxene (Powell & Holland, 1999), Cpx for clinopyroxene (HP) (Holland & Powell, 1996), Ilm(WPH) for ilmenite (White *et al.*, 2000), melt(HP) for melt (Holland & Powell, 2001; White *et al.*, 2001), Mt(W) for magnetite (Wood *et al.*, 1991), Sp(HP) for spinel (Holland & Powell, 1998). Melt loss was set to occur when a 7 vol.% threshold of melt was exceeded and extraction left 1 vol.% behind approximating melt retained on grain boundaries.

The Gibbs free energy minimisation method only considers discrete variation between arbitrary subdivisions within solid solution phases (pseudocompounds) with linear interpolation. Consequently, only a finite number of different phase proportions are produced resulting in slight variations in stable phase assemblages and their proportions between similar *P-T* conditions. Variation of stable phase assemblages introduce artefacts into pseudosections (Fig. 4a) while contrasting phase proportions at similar *P-T* conditions can offset threshold events blurring further boundaries (Fig. 7a). To alleviate these issues, we devised an approach called *threshold buffering*. *Threshold buffering* works by forcing the first time triggering of a threshold event to be postponed by a set number of points ensuring that the threshold is only triggered when it is consistently exceeded. The buffer is reset each time the threshold fails to be triggered (thus all boundaries are shifted by equal amounts). A resolution of 2 °C per point was used and a *threshold buffering* of 1 point (the system postpones extraction by 2 °C).

4.3. Comparing the results

Rcrust can output wt.%, mol.% or vol.% proportions. However, since volumes are pressure dependent plotting wt.% graphs yielded results most consistent with the case study (Fig. 4b & c). Phase proportions for the simple clockwise *P-T* paths show good agreement between the

simulations of Yakymchuck & Brown (2014) and that of Rcrust (Fig. 4b & c). Similar melt proportions are extracted at corresponding points on each P - T path. Minor differences are found for phase stabilities with Rcrust predicting clinopyroxene from 660 to 700 °C and a lower temperature sillimanite in boundary. These discrepancies are attributed to the difference in solution models chosen and updates in the thermodynamic dataset. However a key difference between the calculation methods is Rcrust's automated handling of a changing bulk composition

4.4. Clockwise P - T path

Each dependent path in Rcrust traverses a single line in P - T - X space and is not limited by the simple binary compositional range inherent to P - T , T - X or P - X diagrams. Individual paths allow investigation of phase proportions, compositions and the changing of a bulk composition through *path-dependent* mode diagrams. To display the advanced functionality this provides, a clockwise P - T path is investigated with the same starting composition (Table 1), chemical system, solution models, 7 vol.% melt threshold, 1 vol.% melt retention and 1 point *threshold buffering* as used in Figure 4c. The clockwise P - T path (Fig. 5a) starts off with the same prograde heating segment as the high pressure (HP) path of Yakymchuck & Brown (2014) from 660 °C, 12 kbar to 860 °C, 18 kbar. This is followed by a retrograde P - T curve similar to those found by O'brien & Rötzler (2003) with near-isothermal decompression to 800 °C, 10 kbar and retrograde cooling until 550 °C, 6kbar. In Rcrust the entire clockwise P - T path is calculated in one simulation with automated bulk compositional changes and variations in P - T segments.

Phase proportions in the open system (Fig. 5e) show that melt loss decreases the ability of the reactive subsystem (RS) to form muscovite or increase the mode of biotite upon decompression. The solidus in the open system is crossed at 820 °C 12.8 kbar as opposed to 680 °C, 6.7 kbar in the closed system. This stabilises phase proportions along the retrograde path resulting in a fluid-absent subsolidus assemblage that preserves garnet, alkali-feldspar and a larger amount of sillimanite/kyanite (Fig. 5e). Only two melt loss events occur on the P - T path, both at early stages of decompression, cumulating a total of 13 wt.% melt in the extract subsystem (ES). To simulate the effects of local magma segregation, where magmas become chemically isolated from the reactive subsystem but remain in a relatively close position in the crust, the extract subsystem is calculated under the same P - T conditions of the reactive subsystem (RS) (Fig. 5f). Here the solidus is encountered at the onset of retrograde

cooling at 800 °C, 12 kbar forming a fluid-present subsolidus assemblage dominated by plagioclase feldspar, quartz, alkali-feldspar and orthopyroxene with minor amounts of muscovite, garnet and/or biotite at low temperatures (Fig. 5f).

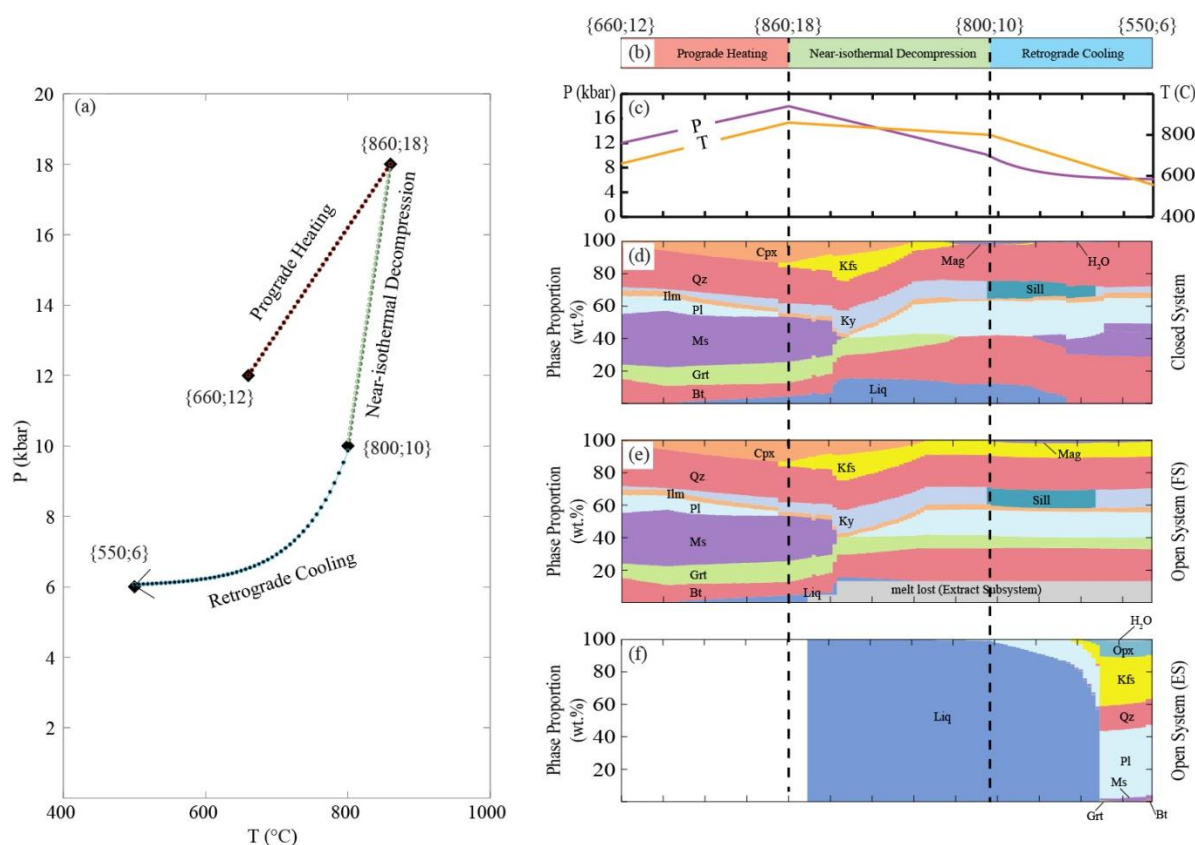


Fig. 5 - (a) Clockwise P - T path consisting of a prograde heating segment from 660 °C, 12 kbar to 860 °C, 18 kbar; followed by near-isothermal decompression to 800 °C, 10 kbar and retrograde cooling until 550 °C, 6kbar. P - T values in Rcrust can be assigned by individual points or as functions of the number of steps in a P - T segment. Thus the prograde heating and near-isothermal decompression segments were assigned values by linear functions of the form $y = ax + y_0$ where y_0 is the initial value and a is the gradient of the segment. The retrograde cooling segment was assigned values by an exponential function of the form $y = -b/c(1-e^{-cx}) + y_0$ where b and c are coefficients, y_0 is the initial value and e is Euler's number. Black diamonds show P - T conditions given in curly brackets as $\{T (^{\circ}\text{C});P (\text{kbar})\}$. Circular dots along each path show individual calculation points in Rcrust. (b) P - T segments with start and end P - T conditions for the clockwise P - T path. (c) Pressures (P) in purple and Temperatures (T) in orange, attained along segments of the clockwise P - T path. (d-f) Phase proportions along the clockwise P - T path for (d) the closed system; (e) the open system (Full System) and (f) the open system (Extract Subsystem). Weight percentages are given relative to the Full System (FS) for (d & e) and only relative to the Extract Subsystem (ES) for (f). Abbreviations for rock forming minerals were taken from Whitney & Evans (2010) and are described in Figure 4.

4.5. Multi-path functionality

The compilation of multiple P - T - X paths can be used to create composite *path-dependent* P - T mode diagrams where a plane in P - T space is filled with points originating from dependent paths. These diagrams are limited to considering paths that are parallel in P - T space as the adjacency of points in the P - T plane must be maintained for readable outputs (when viewing the P - T plane orthogonally points cannot overlap).

This compilation method works by placing each point in a P - T - X path as sequential points in the column of a matrix. Each P - T - X path is placed in a new column. Starting conditions, bulk compositions and P - T - X event parameters can be scaled across the columns. Stable phase assemblages for each point are calculated and each unique assemblage is assigned an identification number.

The simplest form of these diagrams is when bulk composition remains constant across all P - T - X points, thus creating a normal P - T pseudosection. However, the Rcrust method is not restricted to keep bulk composition constant. Pressure, temperature and bulk composition can vary simultaneously within each P - T - X path allowing unique values to be attained dependent on the path taken. *Path-dependence* requires the diagrams be read in the direction of their constituent vectors, as events along the paths are not necessarily reversible on the path or scalable across paths. For example, when dealing with bulk compositional changes by melt loss events, we cannot assume that change through heating can be restored by cooling, nor can we assume that heating followed by decompression will result in the same bulk composition as decompression followed by heating. Points within a path are dependent on previous values therefore have to be determined in sequence. However if paths are set to be independent of one another they can be run in parallel threads to allow multiple calculations in the same simulation time.

4.6. Exploring new functionality

Multi-path functionality allows an array of isobaric heating paths to be examined. Melt loss events alter the bulk composition along the dependent paths, curving the P - T plane in the X dimension creating a *path-dependent* P - T mode diagram (Fig. 6d). The *path-dependent* P - T mode diagram in this case is dependent on bulk compositional changes encountered along the array of its constituent isobaric heating paths (grey arrows in Fig. 6d). For each point in the diagram, the amount of H_2O depends on the cumulative bulk compositional changes

encountered by all points on the path before it. However each point on a path, is unaffected by points on adjacent paths. Thus the dependence of points relies on the direction of their constituent vectors. The reader must take note of the direction of the vectors and should be warned against false interpretations. These new *path-dependent P-T* mode diagrams provide a powerful tool which enables us to investigate the concepts proposed by Yakymchuck & Brown (2014) in more depth.

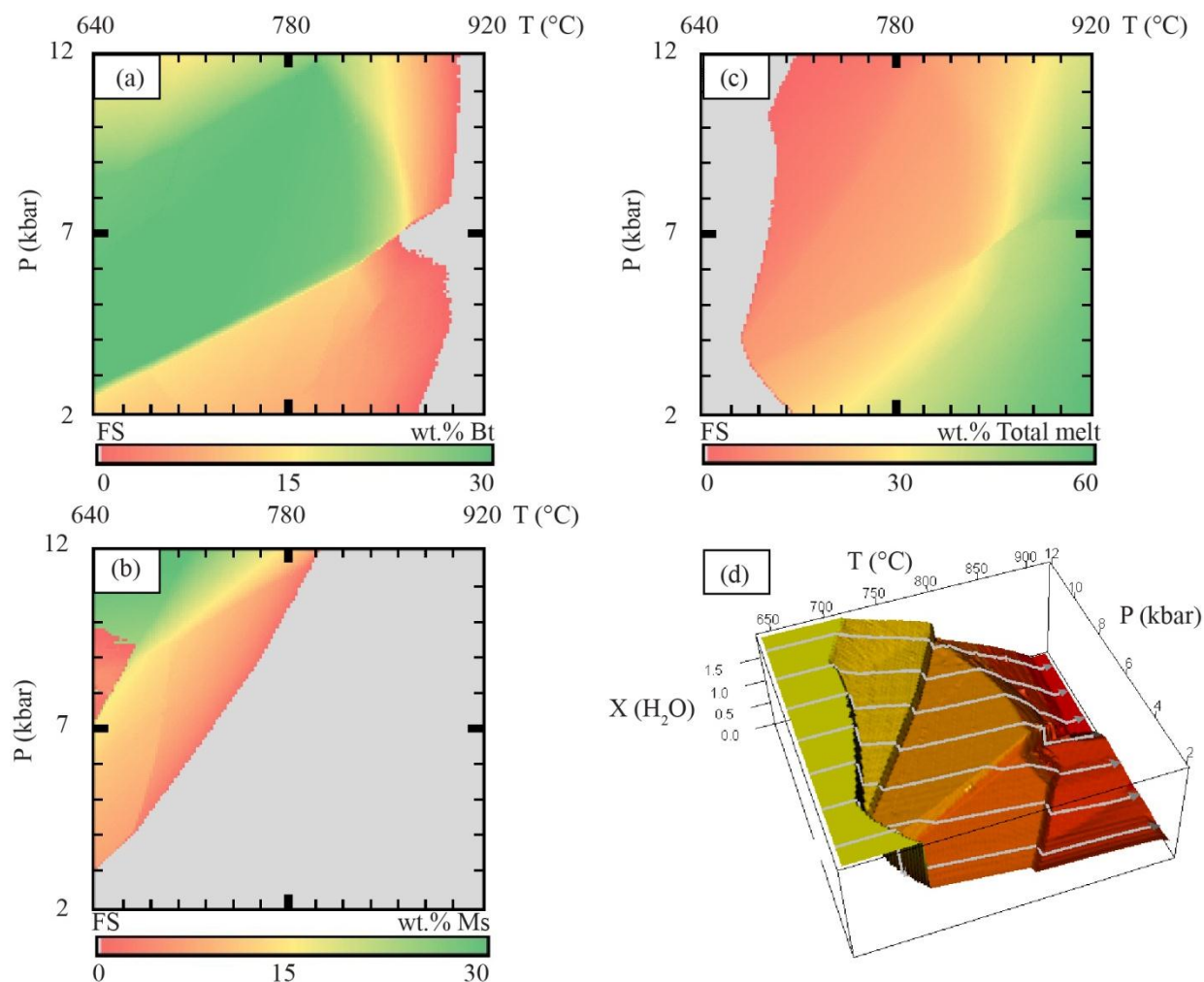


Fig. 6 - Contour plots of weight percentage (a) biotite, (b) muscovite and (c) total melt in the full system for the closed system case. Values of zero are highlighted in grey for clarity. Contour values are given relative to the full system (FS) as indicated on the lower left hand side of each diagram. (d) *Path-dependent P-T* mode diagram from the compilation of isobaric heating paths starting with the composition in Table 1 at 640 °C followed by heating to 940 °C. Melt loss occurs whenever a 7 vol.% threshold is exceeded and leaves behind 1 vol.% melt approximating melt retention on grain boundaries. Grey arrows show the direction of constituent vectors (the isobaric heating paths). X scales the amount of H₂O in the bulk composition of the reactive subsystem. Colour shading is applied on the X variable with yellow close to 2 wt.% H₂O and red close to 0 wt.%

5. RESULTS – EFFECTS OF MELT LOSS

5.1. Isobaric heating (IBH)

A *path-dependent P-T* mode diagram is created with melt extraction defined to occur whenever a 7 vol.% threshold is exceeded. When melt extraction is triggered all melt present in the reactive subsystem (RS) is extracted down to 1 vol.%. This approximates melt retention on grain boundaries. The melt extracts are stored in the extract subsystem (ES) that is independent from further *P-T-X* change and chemically isolated from the reactive subsystem. The same starting bulk composition, chemical system and solution models are used as described above. The *path-dependent P-T* mode diagram is built by combining parallel isobaric heating (IBH) paths from 2 to 12 kbar on the y-axis with a resolution of 141 paths each containing 141 points that span 640 to 920 °C on the x-axis (2 °C and 0.07 kbar per point with a *threshold buffering* of 1 point)(Fig. 7). These IBH mode diagrams can only be read from low temperature to high temperature as they are created by heating at fixed pressures. This is shown by the vector orientation at the top of Figs. 7, 9 & 10).

5.1.1. IBH interstitial melt

The amount of melt in the reactive subsystem (thus the interstitial melt) is contoured in Fig. 7a. The solidus is found on the left hand side of the diagram and is curved due to the pressure dependence of dissolved H₂O in melt. For pressures above 6 kbar, the amount of interstitial melt increases gradually up temperature to a local maximum at the boundary of the first threshold event (Fig 7a green contour with a positive slope intersecting at 780 °C, 12 kbar). At this boundary the interstitial amount exceeds the melt threshold of 7 vol.% so all melt except 1 vol.% is extracted. Heating beyond this boundary causes further melting and more extraction events producing a striped pattern of interstitial melt contours.

The low pressure range (<5 kbar) produces contrasting interstitial melt amounts at adjacent pressures. Areas which exceeded the threshold by a larger amount extract more interstitial melt initially which hinders further melting introducing lags in interstitial melt build up. This effect knocks on to points further along the path blurring the boundaries between extraction events at high temperatures and low pressures. As explained earlier this effect is somewhat lessened by the use of *threshold buffering*.

5.1.2. IBH total melt

The sum of the interstitial melt and the cumulative melt extracted along each path gives the total melt produced by the isobaric heating paths (Fig. 7b). Volume is pressure and temperature dependent necessitating the summing of melt extracts from a variety of *P-T*

conditions to be done on a mass basis. As a result the contour of total melt is plotted as the wt.% of melt relative to the full system (FS). The full system in this simulation consists of the reactive subsystem (RS) and the extract subsystem (ES). Contours scale total melt from close to 0 wt.% as red to 40 wt.% as green with null values highlighted in grey. The largest amount of total melt is found at the highest temperatures and lowest pressures. Contour shapes closely match that of the closed system total melt (Fig. 6c) but have a significant reduction in magnitude from a maximum of 60 wt.% to a maximum of 40 wt.%.

5.1.3. IBH residuum bulk H₂O

For the *P-T-X* space investigated the bulk H₂O content of the residuum is a major control on its subsequent fertility. The amount of H₂O in the bulk composition of the reactive subsystem (RS) is contoured from close to 0 wt.% as red to 2 wt.% as green. Minimum residuum bulk H₂O occurs at mid to high pressures (8 to 11 kbar) and the highest temperatures modelled (Fig. 6c).

5.2. Isothermal decompression (ITD)

To complete the simple clockwise *P-T* investigation by Yakymchuck & Brown (2014) an isothermal decompression (ITD) *path-dependent P-T* mode diagram is created by projecting an array of parallel decompression paths down pressure from the 12 kbar isobaric heating path (IBH12). In these diagrams each point (for example the point at 780 °C, 7kbar in Fig. 7d) is reached by first following isobaric heating at 12 kbar until the point's temperature (here 780 °C) followed by isothermal decompression until the points pressure (here 7kbar). Thus points in the diagram can only be read going down pressure as shown by the vector orientation at the top of Figs. 7, 8, 9 & 10.

Melt extraction along the heating and decompression paths are defined by the same 7 vol.% threshold, 1 vol.% melt retained on grain boundaries and 1 point *threshold buffering* as in the IBH system. Melt is extracted along the IBH12 path as well as along each respective ITD path so an indication of the melt lost during the isobaric heating path is placed above the diagram (Fig. 7d). Melt lost is summed cumulatively on a weight basis and calculated relative to the full system (FS). Extraction events change the starting composition of decompressing paths, so for clarity in listing observations, the *P-T* space is classified into fields (with roman numerals) based on the amount of melt loss. The field bounds are: I (no melt loss) 640-780 °C; II (5 wt.%) 780-800 °C; III (10 wt.%) 800-840 °C; IV (15 wt.%) 840-870 °C, V (20 wt.%) 870-900 °C and VI (25 wt.%) >900 °C

5.2.1. ITD interstitial melt

Interstitial melt in Fig. 7d is contoured with the same scale as Fig. 7a to allow direct comparison. IBH12 melt loss fields are indicated with roman numerals. Boundaries to decompression melt extraction events occur at high angles to the constituent paths.

Paths that originate from the IBH12 path at temperatures below 800 °C have experienced 5 wt.% or less melt loss on the heating path (Fig. 7d I and II). These paths, upon decompression, show sequential melting zones bounded by melt thresholds.

Paths that originate above 800 °C have lost more than 5 wt.% melt on the IBH12 path. Melt loss events here break the interstitial melt contours into discrete fields which correspond with the IBH12 melt loss fields. Each of these fields starts off with melt present at 12kbar and has larger amounts of melt towards their respective high temperature boundaries. Decompression from 12 to 8 kbar, for fields between 800 and 900 °C (Fig. 7d III-V), decreases the amount of interstitial melt present. The decrease in interstitial melt upon decompression creates zones in *P-T* space where all melt in the reactive subsystem is crystallised. Melt is only encountered again after further decompression across a positively sloped line that intersects around 7.5 kbar and 920 °C. The >900 °C field (Fig. 7d VI) shows a slight increase in melt during decompression up to 7.5 kbar after which no interstitial melt is present until 2 kbar.

5.2.2. *ITD total decompression melt*

To highlight changes in decompression melt production the interstitial melt encountered along the ITD paths is summed with only the melt extracted during decompression (not including melt extracts from the IBH12 path)(Fig. 7e). Thus the total melt for each point in the *P-T* space can be found by adding the total decompression melt (Fig. 7e) to the IBH12 melt loss (above Fig. 7d). The maximum cumulative decompression melt formed in the given *P-T* space (~25 wt.%.) is found at 2 kbar at the high temperature end of the 780-800 °C field (Fig. 7e II). The >900 °C field (Fig. 7eVI) does not experience melt loss events along any of its respective decompression paths.

5.2.3. *ITD residuum bulk H₂O*

Decompression of the residuum at low total IBH12 melt loss (e.g. <800 °C Fig. 7f I & II) shows a systematic reduction in its bulk H₂O content. Higher temperatures are associated with more IBH12 melt loss and less decompression melt loss. Therefore decompression at higher temperatures has less of an effect on the residual bulk H₂O content. The lowest bulk H₂O content is found in the >900 °C field (Fig. 7f VI) at ~0.07 wt.%. This value is constant from 900 °C up temperature and down pressure as there are no decompression melt loss events in this field.

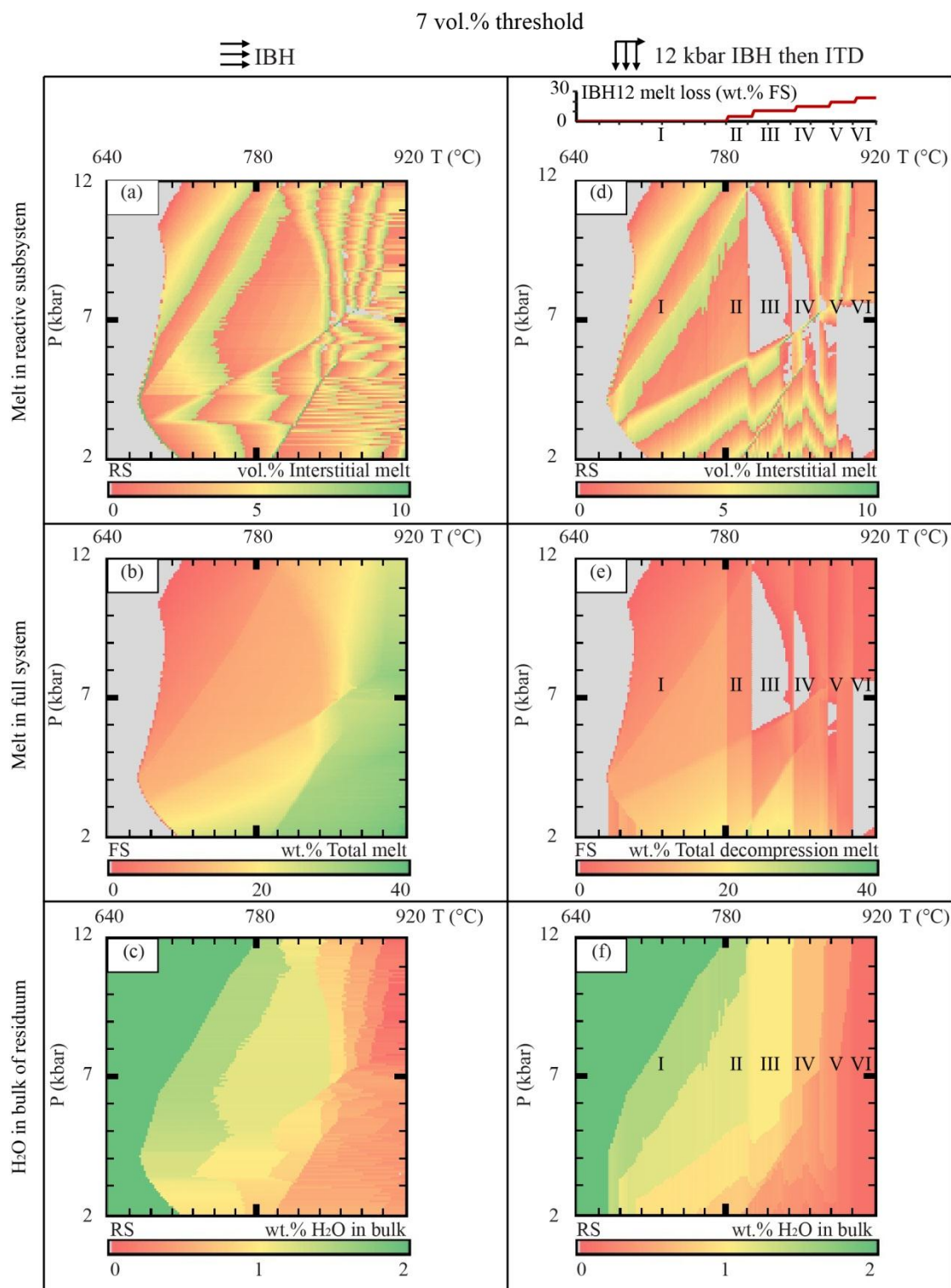


Fig. 7 - 7 vol.% threshold *path-dependent P-T mode diagrams* showing: (a,d) volume percentage melt in the reactive subsystem (interstitial melt); (b,e) weight percentage melt in the full system (total melt); (c,f) weight percentage of H₂O in the bulk composition of the reactive system (residuum) for the isobaric heating system (IBH)(a-c) and the 12kbar isobaric heating followed by isothermal decomposition system (ITD)(d-f). Values of zero are highlighted in grey for clarity. Contour values are given relative the reactive subsystem (RS) or the full system (FS) as indicated on the lower left hand side of each diagram.

5.3. Melt crystallisation zones

The close correlation between the bulk H₂O content of the reactive subsystem and the amount of interstitial melt in the reactive subsystem suggests, for this system at least, that H₂O is a limiting factor for melt production. In order to try explain the interesting decompression melt behaviour exhibited by the 7 vol.% threshold ITD system, the phase boundaries of the H₂O bearing phases muscovite, biotite and cordierite are plotted along with garnet and alkali-feldspar (Fig 8). The presence of interstitial melt is indicated by stippling and the garnet-biotite difference (the abundance of garnet minus the abundance of biotite both relative to the reactive subsystem) is contoured (Fig 8).

Heating along IBH12 initiates *muscovite melting* after 700 °C consuming muscovite, plagioclase and quartz (Fig. 8). At 12 kbar this melting produces only two melt extraction events (at 780 and 800 °C; Fig. 8 II & III) up to the muscovite-out-line at 800 °C. Cumulatively these events yield a maximum of 10 wt.% melt (Fig 8, Fig6 d). Further heating along IBH12 causes *biotite melting* (consuming biotite, plagioclase and quartz) across 3 melt extraction events (Fig. 8 IV-VI) forming a further 15 wt.% melt.

Decompression from the IBH12 path in the region before 780 °C encounters two decompression melt loss events due to *muscovite melting* before the muscovite-out-line followed by two decompression melt loss events after the cordierite-in-line where cordierite forms in favour of biotite (Fig. 8 I, Fig. 6d I).

Decompression in the 800-840 °C field (Fig. 8 III, Fig. 7d III) decreases the amount of interstitial melt in the reactive subsystem. This melt crystallisation corresponds to a shift in the garnet-biotite difference from 0 wt.% to -38 wt.%. This is thought to be the result of the thermodynamic system, upon decompression, using the H₂O budget of the system to form biotite at the expense of garnet and melt. After all the melt has crystallised the system continues to consume garnet (though in relatively smaller volumes for equivalent amounts of decompression) until the garnet-out-line around 7.5 kbar. Thus decompression melting in the 800-840 °C field (Fig. 8 III, Fig. 7d III) is only encountered again after 6 kbar of decompression when the cordierite-in-line is met.

Below the cordierite-in-line, cordierite and melt form in favour of biotite. Thus the high temperature side of the 800-840 °C field (Fig. 8 III) encounters a region where biotite, garnet, cordierite and melt coexist. The garnet-biotite difference in this region shows a shift from values near 0 wt.% to values close to -15 wt.% followed by an area of melt crystallisation. This shows again that if biotite, garnet and melt are present the system prefers biotite formation in favour of garnet thus melt crystallises upon decompression. This process

continues down pressure until all biotite is consumed at around 4 kbar (biotite-out-line)(Fig. 8 III).

Decompression in the 840-870 °C and 870-900 °C fields (Fig. 8 IV & V) encounter similar features however there is a greater abundance of biotite and lesser abundance of garnet thus shifts in the garnet-biotite difference are less drastic and a smaller amount of melt is crystallised.

In the field >900 °C (Fig. 8 VI) melt is the only H₂O bearing phase above 7.5 kbar. Melt at lower pressures incorporates a lower amount of dissolved H₂O consequently decompression produces melting until the cordierite-in-line. Decompression across this boundary causes cordierite formation in favour of melt.

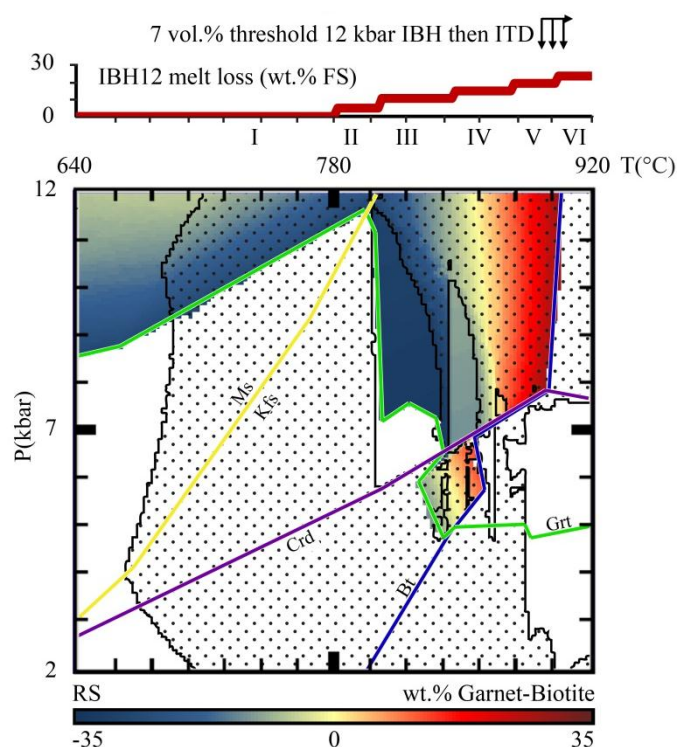


Fig. 8 - Phase boundaries and garnet-biotite mode difference for the 7 vol.% threshold 12kbar isobaric heating followed by isothermal decompression system (ITD). Melt lost along the 12 kbar isobaric heating path (IBH12) is given above the main diagram as weight percentage relative to the Full System (FS). The temperature space is divided into zones based on the amount of melt extracted along IBH12 which are assigned roman numerals up temperature as: I (no melt loss) 640-780 °C; II (5 wt.%) 780-800 °C; III (10 wt.%) 800-840 °C; IV (15 wt.%) 840-870 °C, V (20 wt.%) 870-900 °C and VI (25 wt.%) >900 °C. On the main diagram garnet-biotite mode difference is contoured as weight percentage of the reactive subsystem (RS) from -35 wt.% difference (blue) where more biotite is present than garnet, through 0 wt.% difference (yellow) to 35 wt.% difference (red) where more garnet is present than biotite. The stippled area shows the presence of melt in reactive subsystem (RS). Boundaries of the garnet (green), muscovite/ alkali-feldspar (yellow), biotite (blue) and cordierite (purple) stability fields are shown as solid lines with labels placed on the side of the line where each phase is present.

5.4. Lower melt threshold investigation

If a lower melt threshold is considered, melt loss events will be more frequent but less voluminous, simulating a fractional melting scenario. If the melt threshold is equal to the melt retention amount, simulations will more closely approximate a ‘bleeding off’ of melt once a connectivity transition is formed as opposed to pulses of melt that break the threshold (a batch melting scenario). To compare these behaviours *path-dependent P-T* mode diagrams are created with melt threshold and melt retention on grain boundaries both set to 1 vol.% (Fig. 9). For both the heating and decompression segments in these diagrams whenever 1 vol.% melt is exceeded all melt is extracted except 1 vol.%. The same *P-T* space, step size and *threshold buffering* is used as stated previously.

5.4.1. IBH interstitial melt (1 vol.% threshold)

Melt volumes exceed the threshold at the solidus attaining their maxima along its boundary (Fig. 9a). This triggers extraction which maintains a near constant 1 vol.% plane throughout the *P-T* space. Clusters of points at high temperature and mid to high pressures show melt crystallisation. Melt crystallisation is also found along the positive sloped cordierite-in-line (Fig. 8).

5.4.2. IBH total melt (1 vol.% threshold)

Total melt contours for 1 vol.% threshold (Fig. 9b) are near identical to that of the 7 vol.% threshold (Fig. 7b) with only a slight decrease in values at higher temperatures. A key difference however is that the melt extract contour (Supplementary Fig. 4b) is largely free of the distortions that are present in the 7 vol.% threshold melt extract contour (Supplementary Fig 2b). This is a result of the lower threshold having more frequent melt loss events so small offsets in *P-T-X* position of these events becomes less important. *Threshold buffering* is thus no longer necessary but is maintained at 1 point *threshold buffering* (2 °C and 0.07 kbar) for consistency between simulations.

5.4.3. IBH residuum bulk H₂O (1 vol.% threshold)

Figure 9c shows that a lower threshold again has a smoothing effect where small pressure offset positions of extraction events are compensated by the multitude of events thereby preventing large knock on distortions seen at high temperatures in the 7 vol.% threshold plots (Fig 7c).

5.4.4. ITD interstitial melt (1 vol.% threshold)

IBH12 melt loss produces a more continuous accumulation of melt with constant gradients of melt loss maintained across the fields delineated by the 7 vol.% threshold system (above Figs.

7d and 9d). A relatively flat gradient of melt formation occurs between 700 and 800 °C (above Fig. 9d I and II) attaining a cumulative maximum of ~6 wt.% melt lost. This is followed by a sharp accumulation of melt at the muscovite-out-line up to 10 wt.% (Fig. 8, above Fig. 9d II). The 800-900 °C region shows a constant gradient across the fields III to V (above Fig. 9d) peaking at 23 wt.%. The gradient of the 800-900 °C region is steeper than the 700 to 800 °C region. The >900 °C field (Fig. 9d VI) shows an almost flat line with no further appreciable melt loss (maintaining a cumulative 23 wt.%).

Isothermal decompression (Fig. 9d) produces a similar 1 vol.% plane to IBH with a matching positive sloped line of melt crystallisation points on the cordierite-in-line (Fig. 8). At temperatures above 800 °C (>5 wt.% IBH12 melt loss) large melt crystallisation fields are found at 800-880 °C, 6-12 kbar and at 860-920 °C, 2-8 kbar. Melt volumes exceeding 1 vol.% occur on the low pressure boundaries of the first field. This occurs because the melt threshold is rapidly exceeded and *threshold buffering* only allows extraction one step after triggering of the threshold.

5.4.5. ITD total decompression melt (1 vol.% threshold)

Smaller more numerous melt loss events are encountered by the 1 vol.% threshold along IBH12 with a more incremental changing bulk composition. This more incremental change causes a more consistent reduction in decompression melt production with increasing temperature (Fig. 9e). Along the 2 kbar line, where the maximum amount of decompression melting has occurred along each respective path, the total decompression melt increases from 670 to 800 °C and then decreases from 800 to 920 °C. Maximum decompression melt is attained at 800 °C with ~23 wt.% (Fig. 9e). Melt crystallisation fields from the interstitial melt plot are still visible but are broken by vertical bands of constant amounts of melt by paths which exceeded the melt threshold before melt crystallisation began.

5.4.6. ITD residuum bulk H₂O (1 vol.% threshold)

Residuum bulk H₂O contents exhibit banding with vertically constant contents below 8 kbar for temperatures above 890 °C and in the area 800-880 °C 6-12 kbar as no melt loss events occur in these regions. Apart from banding and a small region below the closed system solidus where decompression paths maintain their melting history (by having lower bulk H₂O contents) the ITD system shows similar patterns to the IBH case (Fig. 9c and f).

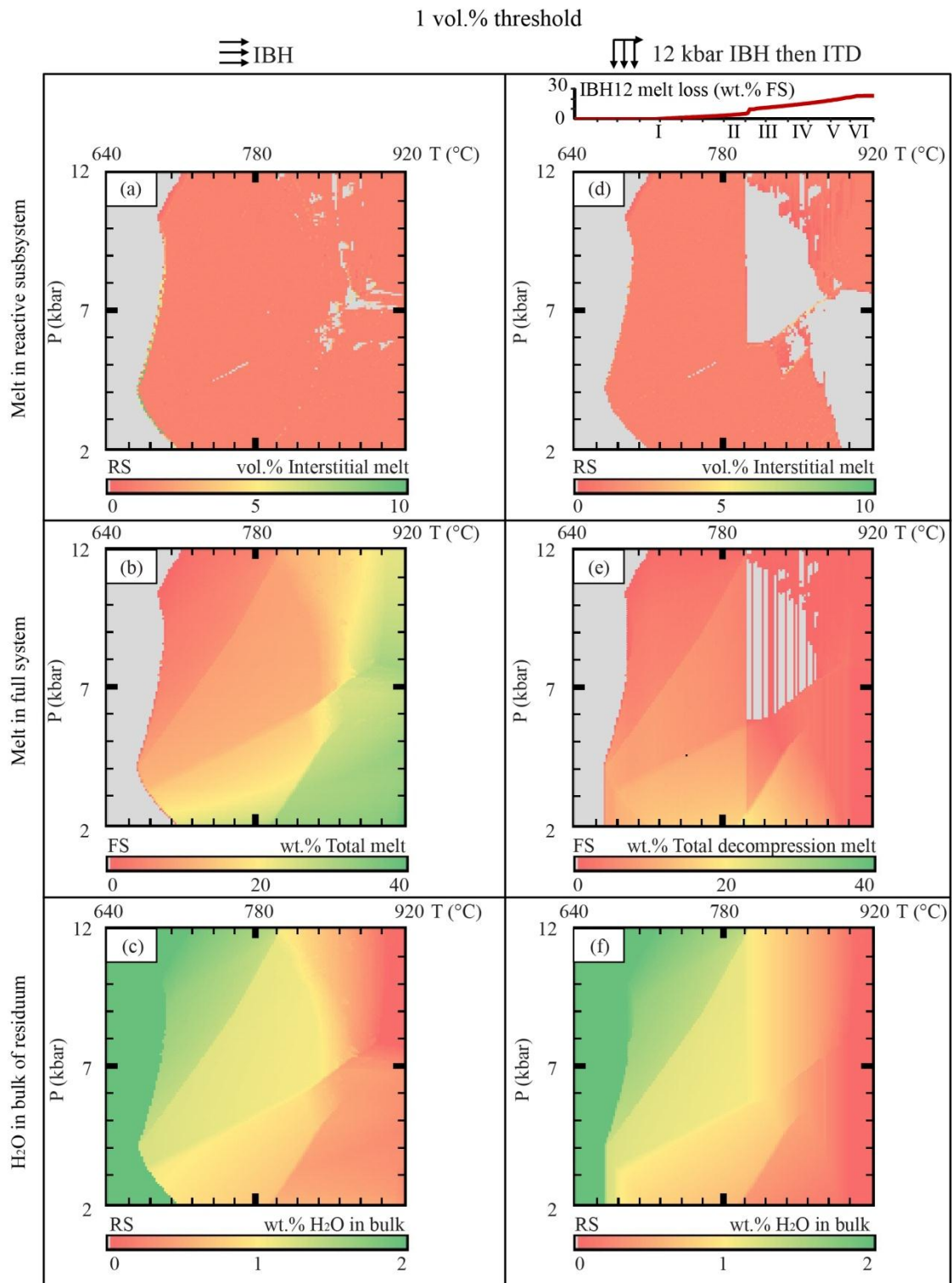


Fig. 9 - 1 vol.% threshold *path-dependent* *P-T* mode diagrams showing: (a,d) volume percentage melt in the reactive subsystem (interstitial melt); (b,e) weight percentage melt in the full system (total melt); (c,f) weight percentage of H_2O in the bulk composition of the reactive system (residuum) for the isobaric heating system (IBH)(a-c) and the 12kbar isobaric heating followed by isothermal decompression system (ITD)(d-f). Values of zero are highlighted in grey for clarity. Contour values are given relative the reactive subsystem (RS) or the full system (FS) as indicated on the lower left hand side of each diagram.

5.5. Melt productivity

The *path-dependent P-T* mode diagrams presented show that for the given pelite starting composition the open system produces less total melt than the closed system. To quantify the difference in productivity, the total melt produced by each open system case (Fig. 10 a & b) is subtracted from that of the closed system (Fig. 6c) and then expressed as a weight percentage difference yielding the *melt productivity difference* (Fig. 10c & d). For isothermal decompression: total melt is the sum of IBH12 extracts, ITD extracts and interstitial melt. *Melt productivity difference* plots for 7 vol.% and 1 vol.% thresholds are similar thus only the 1 vol.% threshold plots are shown (Fig. 10).

Positive *melt productivity differences* show areas where the open system has produced more melt than the closed and negative values where the closed system has produced more than the open. A few positive *melt productivity difference* values are found however these only occur near the closed system solidus where uncertainty in melt amounts are greatest with the difference in melt amount too small to be considered significant. The vast majority of *melt productivity differences* are negative scaling from close to 0 wt.% as white to -40 wt.% as dark red.

For low total amounts of melting ($P > 3$ kbar in the *muscovite melting* region and $P < 3$ kbar in the cordierite formation region, Fig. 8) open systems are as productive as closed systems with *melt productivity differences* of around 0 wt.% (Fig. 10). The onset of *biotite melting* down pressure from the cordierite-in-line or up temperature from the muscovite-in-line produces a range of negative *melt productivity differences* (Figs. 8 & 10). *Melt productivity differences* achieve local minima at the biotite-out-line (most distinct at pressures below the cordierite-in-line) decreasing again to global minima at the high temperature end of the biotite-absent- zones (Figs. 8 & 10). The IBH12 followed by ITD case attains lower productivities with a minimum of -38 wt.% *melt productivity difference* as opposed to the IBH case with -27 wt.%.

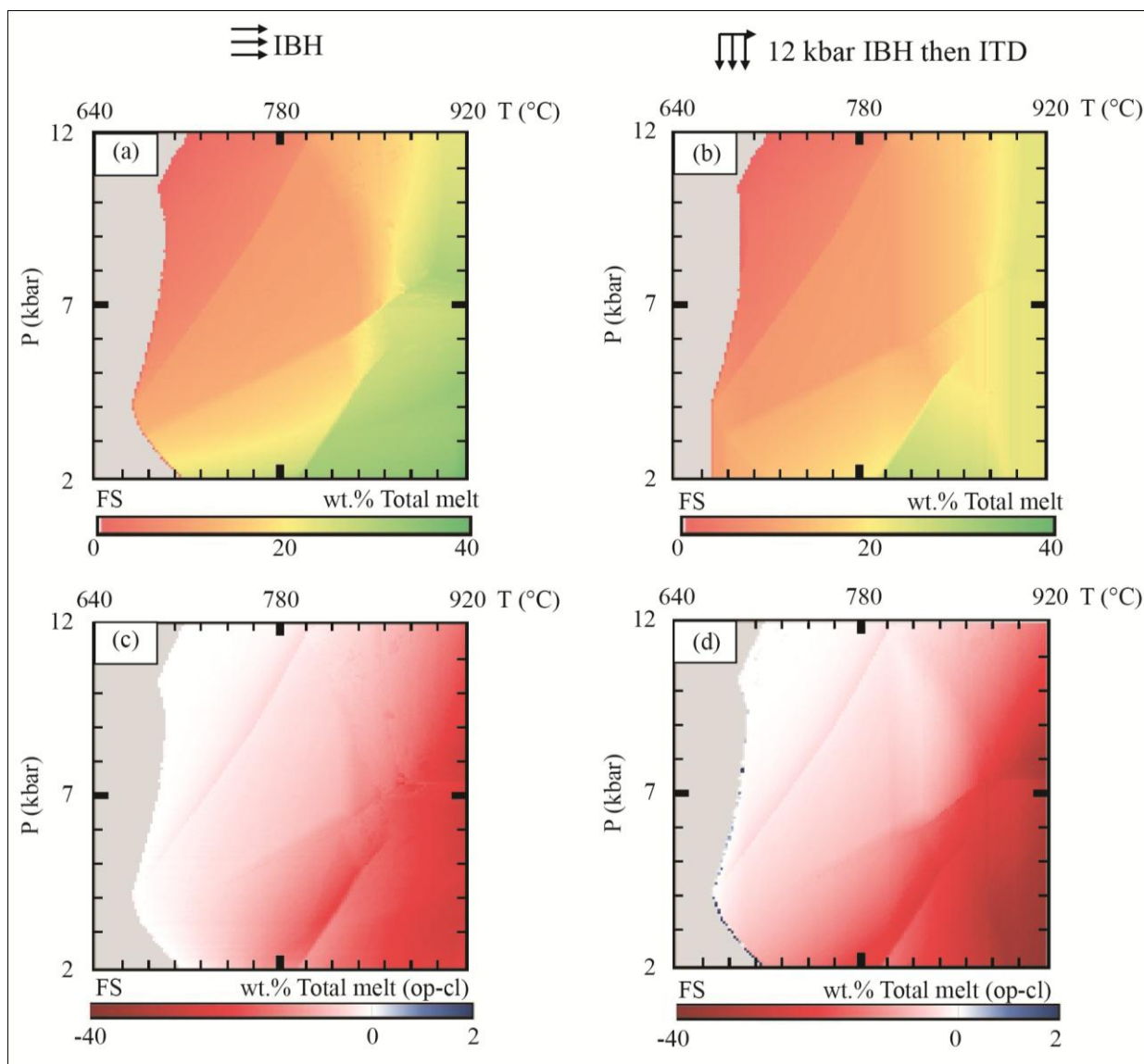


Fig. 10 - 1 vol.% threshold *path-dependent* P - T mode diagrams showing: (a) total melt in the open isobaric heating system (IBH) (b) total melt for the 12 kbar isobaric heating followed by isothermal decompression system (ITD) as the sum of total decompression melt and melt lost along the 12 kbar isobaric heating path (IBH12). *Melt productivity difference* contours calculated by subtracting the total melt produced by the closed system (Fig. 6c) from that of the open IBH system (a & c) and the open ITD system (b & d). If the open system is more productive than the closed a positive value is attained, scaling here from white to blue as 0 to 2 wt.%. If the open system is less productive than the closed a negative value is attained, scaling here from white to red as 0 to -40 wt.%. *Melt productivity differences* of precisely zero only occur subsolidus in these diagrams so are highlighted in grey for clarity. *Melt productivity difference* contours for 7 vol.% threshold are indistinguishable from that of 1 vol.% so only the latter are shown here. Contour values are given relative to the full system (FS) as indicated on the lower left hand side of each diagram.

6. DISCUSSION

6.1. Effects of melt loss

The H₂O content of a suprasolidus rock has a major influence on its fertility. Rocks in the mid- to lower-crust have low porosities; consequently they contain minimal H₂O at the solidus (White & Powell, 2002). The starting bulk composition investigated in this study (Table 1) is accordingly adjusted to be fully hydrated but with only a small proportion of free fluid (<0.1 mol*.% free H₂O) just below the solidus. However this adjustment is made specifically for a pressure of 12 kbar. Thus paths in the IBH system that intersect the solidus at pressures below 12 kbar will have too much free water which will lead to an overestimate of melt production. Paths in the ITD system are free of these distortions as their starting bulk compositions are derived from the IBH12 path.

A lower melt threshold for extraction events restricts the fluctuation of interstitial melt in the reactive subsystem but results in similar generalised trends for total IBH melt (Figs. 7b & 9b) and the resultant residuum bulk H₂O (Figs. 7c & 9c). The ‘smoothing’ effect of a lower threshold is attributed to there being more numerous but less voluminous extraction events thus pressure differences have less of a knock on effect.

Contours of total melt for the closed and open systems show that melt loss decreases total melt production (Figs. 6c, 10a & b). This implies that open systems are less melt productive than closed, as shown and reported by Yakymchuck & Brown (2014). Melt loss events during *muscovite melting* (<800 °C, >3 kbar) and low temperature *biotite melting* (<800 °C, < 5 kbar) produce relatively small amounts of melt (generally < 20 wt.% of the full system (FS))(Figs. 6c, 10a & b). At these low temperatures (<800 °C) bulk compositional change induced by the cumulative loss of melt has little effect on total melt production. We see this as *melt productivity differences* remain close to 0 wt.% (achieving an average minimum of -7 wt.% for IBH and -8 wt.% for ITD at 800 °C)(Fig. 10).

At temperatures above 800 °C for IBH systems cordierite absent (>8 kbar) and cordierite present (<8 kbar) *biotite melting* produces large amounts of melt (cumulative total melt reaching maximums close to 40 wt.%, Fig. 7b & 9b). However these values are significantly lower than that achieved by the closed system (Fig. 6c) where cumulative total melt reaches maximums close to 60 wt.%. This is seen further by *melt productivity differences* for individual paths in the IBH system reaching up to 27 wt.% less melt in the open system than the closed system (Fig. 10c).

ITD systems at temperatures above 800 °C show distinctly different behaviour from that of IBH systems (Figs. 7, 9 & 10). It is found that if garnet, biotite and melt are present upon decompression (as they are between 800-900 °C and 12-8 kbar) then the thermodynamic system uses the H₂O budget of the system to form biotite at the expense of garnet and melt (Fig. 8). This causes zones of melt crystallisation where decompression reduces the amount of melt in the reactive subsystem (Figs. 7d,8 & 9d). Significant amounts of decompression melting can only be achieved after 6 kbar of decompression when cordierite stability is encountered (Fig. 8). Thus the cumulative total melt achieved by the ITD system reaches maxima of only around 30 wt.% (Fig. 10b) and *melt productivity differences* achieve up to 38 wt.% less melt in the open system than the closed system (Fig. 10d).

Total decompression melt increases to the high temperature side of each IBH12 melt loss field but from 800 °C (Figs. 7e & 9e III-V) up temperature each melt loss field attains sequentially lower maxima. This implies that, for regions above 800 °C, melt loss has a larger effect on a residuum's ability to produce melt than increased temperatures has. Thus optimum decompression melt comes from a playoff between high temperatures and low IBH12 melt loss.

For temperatures above 800 °C ITD attains lower total melt and *melt productivity differences* than IBH (Fig. 10) implying that, for the given pelite starting composition in the open system, decompression is less melt productive than heating. Importantly these results only suggest a reduction in residuum fertility; the extract subsystem could contain a combination of solid phases (either entrained or crystallised) that are fertile enough to melt upon decompression.

6.2. Rcrust

The case study and its expansion were chosen for the complicated use of a changing effective bulk composition and use of a thermodynamic calculation method that is independent of Rcrust's. Rcrust uses meemum based minimisation of Gibbs free energy whereas the Yakymchuck & Brown (2014) case study used THERMOCALC's solution of non-linear equations. For singular paths the close correlation between results from Yakymchuck & Brown (2014) and that of Rcrust implies validation for its use in this manner and for simpler cases. As the case study expansion demonstrates, Rcrust provides an efficient tool for modelling with a changing effective bulk composition. The automated handling of

bulk compositional changes allows a closer approximation of open systems as more frequent melt loss events can be considered without becoming prohibitively time consuming to calculate. Multiple applications exist for the new modelling tool presented. These include: the modelling of open system melt loss behaviour, introduction of contaminant phases or fluids, shielding of slow diffusing phases from the effect bulk composition of the reactive subsystem or the setting up of a heterogeneous crustal column with an array of starting compositions that are subjected to a geotherm

7. CONCLUSION

Rocks that lose melt along the prograde path form bulk compositions with lower H₂O concentrations. As H₂O is a major control of fertility the ability of the residuum to produce further melt is hindered. After increased amounts of melt loss, at low pressures and/or high temperatures, the loss in residuum fertility exceeds the amount of melt being extracted therefore open systems become less melt productive than closed systems.

The productivity of the open system can be determined by the combination of initial bulk composition and P - T path taken. The starting bulk composition sets the initial positions of phase stabilities and defines the phases involved in melting reactions. The P - T path taken determines the angle of interception with these reactions and thus the spacing of melt loss events. Pressure dependence of melt's H₂O content influences the volume of melt extracted and the severity in effect of melt loss on the residual system. Melt loss cumulatively depletes residuum H₂O which in turn, amongst other factors, prevents further melt loss. The style of melt loss as either isolated pulses of melt, or as a continuous bleeding off of melt that exceeds the threshold, appears to have negligible impact on the total melt amount (at least for the comparison of 1 and 7 vol.% thresholds in this study).

The case study and its expansion demonstrate the added investigative abilities of Rcrust's simultaneous study of pressure (P), temperature (T) and bulk compositional (X) effects, achieved through *path-dependence*. Stepwise consideration of phase manipulations will allow the future integration of kinetic restraints. Careful consideration of modelling results coupled with experimentation and field relations could create an internally consistent thermodynamically and kinetically constrained model for crustal anatexis. This would provide a major advance for the understanding of crustal differentiation.

ACKNOWLEDGEMENTS

Funding by the South African National Research Foundation (NRF) through the Scare Skills Bursary to M.J. Mayne and from the South African Research Chairs Initiative (SARChI) to G. Stevens is gratefully acknowledged. M.J. Mayne would like to acknowledge support from the European Research Council (project MASE, ERC StG 279828 to J. van Hunen). L. Kaislaniemi acknowledges support from the European Union FP7 Marie Curie Initial Training Network Topomod, contract 264517. JFM wishes to thank V Janousek for introducing him to R coding and making the whole Rcrust possible.

REFERENCES

- Ague, J. J., 1991. Evidence for major mass transfer and volume strain during regional metamorphism of pelites. *Geology*, **19**(8), 855-858.
- Albee, A. L., 1965. A petrogenetic grid for the Fe-Mg silicates of pelitic schists. *American Journal of Science*, **263**(6), 512-536.
- Auzanneau, E., Schmidt, M. W., Vielzeuf, D. & Connolly, J. D., 2010. Titanium in phengite: a geobarometer for high temperature eclogites. *Contributions to Mineralogy and Petrology*, **159**, 1-24.
- Becker, R. A., Chambers, J. M., & Wilks, A. R., 1988. The new S language: a programming environment for data analysis and graphics, Wadsworth and Brooks. *Cole, Pacific Grove*
- Berman, R. G. & Brown, T. H., 1984. A thermodynamic model for multicomponent melts, with application to the system CaO-Al₂O₃-SiO₂. *Geochimica et Cosmochimica Acta*, **48**, 661-678.
- Brown, M. & Korhonen, F. J., 2009. Some remarks on melting and extreme metamorphism of crustal rocks. In: *Physics and Chemistry of the Earth's Interior*, pp. 67-87. Springer, New York.
- Clemens, J. D., 1984. Water contents of intermediate to silicic magmas. *Lithos*, **17**, 273-287.
- Clemens, J. D., 1990. The granulite—granite connexion. In: *Granulites and crustal evolution*, pp. 25-36. Springer, Netherlands.
- Clemens, J. D. & Stevens, G., 2012. What controls chemical variation in granitic magmas?. *Lithos*, **134**, 317-329.

- Coggon, R. & Holland, T. J. B., 2002. Mixing properties of phengitic micas and revised garnet-phengite thermobarometers. *Journal of Metamorphic Geology*, **20**(7), 683-696.
- Connolly, J. A. D., 2005. Computation of phase equilibria by linear programming: A tool for geodynamic modeling and its application to subduction zone decarbonation. *Earth and Planetary Science Letters*, **236**, 524-541.
- Connolly, J. A. D., 2009. The geodynamic equation of state: what and how. *Geochemistry, Geophysics, Geosystems*, **10**.
- Connolly, J. A. D. & Kerrick, D. M., 1987. An algorithm and computer program for calculating composition phase diagrams. *Calphad*, **11**, 1-55.
- de Capitani, C. & Petrakakis, K., 2010. The computation of equilibrium assemblage diagrams with Theriak/Domino software. *American Mineralogist*, **95**(7), 1006-1016.
- Diener, J. F. A., Powell, R. & White, R. W., 2008. Quantitative phase petrology of cordierite–orthoamphibole gneisses and related rocks. *Journal of Metamorphic Geology*, **26**, 795-814.
- Fuhrman, M. L. & Lindsley, D. H., 1988. Ternary-feldspar modeling and thermometry. *American Mineralogist*, **73**, 201-215.
- Ghiorso, M. S. & Sack, R. O., 1995. Chemical mass transfer in magmatic processes IV. A revised and internally consistent thermodynamic model for the interpolation and extrapolation of liquid-solid equilibria in magmatic systems at elevated temperatures and pressures. *Contributions to Mineralogy and Petrology*, **119**, 197-212.
- Gottschalk, M., 1997. Internally consistent thermodynamic data for rock-forming minerals in the system $\text{SiO}_2\text{-TiO}_2\text{-Al}_2\text{O}_3\text{-CaO-MgO-FeO-K}_2\text{O-Na}_2\text{O-H}_2\text{O-CO}_2$. *European Journal of Mineralogy*, **9**(1), 175-223.

- Helgeson, H. C., Delany, J. M. & Nesbitt, H. W., 1978. Summary and critique of the thermodynamic properties of rock-forming minerals. *American Journal of Science* **278A**, 1-229.
- Hensen, B. J. & Essene, E. J., 1971. Stability of pyrope-quartz in the system MgO-Al₂O₃-SiO₂. *Contributions to Mineralogy and Petrology*, **30**(1), 72-83.
- Hensen, B. J. & Harley, S. L., 1990. Graphical analysis of P—T—X relations in granulite facies metapelites. In: *High-temperature metamorphism and crustal anatexis*, pp. 19-56. Springer, Netherlands.
- Holland, T. & Powell, R., 1996. Thermodynamics of order-disorder in minerals: II. Symmetric formalism applied to solid solutions. *American Mineralogist*, **81**, 1425-1437.
- Holland, T. & Powell, R., 1998. An internally consistent thermodynamic data set for phases of petrological interest. *Journal of metamorphic Geology*, **16**, 309-343.
- Holland, T. & Powell, R., 2001. Calculation of phase relations involving haplogranitic melts using an internally consistent thermodynamic dataset. *Journal of Petrology*, **42**, 673-683.
- Holland, T. & Powell, R., 2003. Activity–composition relations for phases in petrological calculations: an asymmetric multicomponent formulation. *Contributions to Mineralogy and Petrology*, **145**, 492-501.
- Holness, M. B. & Sawyer, E. W., 2008. On the pseudomorphing of melt-filled pores during the crystallization of migmatites. *Journal of Petrology*, **49**, 1343-1363.
- Ihaka, R. & Gentleman, R., 1996. R: a language for data analysis and graphics. *Journal of computational and graphical statistics*, **5**, 299-314.

- Janoušek, V., Farrow, C. M. & Erban, V., 2006. Interpretation of whole-rock geochemical data in igneous geochemistry: introducing Geochemical Data Toolkit (GCDkit). *Journal of Petrology*, **47**, 1255-1259.
- Johnson, T.E., Gibson, R.L., Brown, M., Buick, I.S. & Cartwright, I., 2003. Partial melting of metapelitic rocks beneath the Bushveld Complex, South Africa. *Journal of Petrology*, **44**, 789-813.
- Johnson, T. E., White, R. W. & Powell, R., 2008. Partial melting of metagreywacke: a calculated mineral equilibria study. *Journal of Metamorphic Geology*, **26**, 837-853.
- Johnson, T.E., Brown, M. & White, R.W., 2010. Petrogenetic modelling of strongly residual metapelitic xenoliths within the southern Platreef, Bushveld Complex, South Africa. *Journal of Metamorphic Geology*, **28**, 269-291.
- Johnson, T.E., Kirkland, C.L., Reddy, S.M. & Fischer, S., 2015. Grampian migmatites in the Buchan Block, NE Scotland. *Journal of Metamorphic Geology*, **33**, 695-709.
- Korhonen, F. J., Saito, S., Brown, M. & Siddoway, C. S., 2010. Modeling multiple melt loss events in the evolution of an active continental margin. *Lithos*, **116**, 230-248.
- Marchildon, N. & Brown, M., 2002. Grain-scale melt distribution in two contact aureole rocks: Implications for controls on melt localization and deformation. *Journal of Metamorphic Geology*, **20**, 381-396.
- Morfin, S., Sawyer, E.W. & Bandyayera, D., 2014. The geochemical signature of a felsic injection complex in the continental crust: Opinaca Subprovince, Quebec. *Lithos*, **196**, 339-355.
- Morse, S. A., 1984. Cation diffusion in plagioclase feldspar. *Science*, **225**, 504-505.
- O'brien, P.J. & Rötzler, J., 2003. High-pressure granulites: formation, recovery of peak conditions and implications for tectonics. *Journal of Metamorphic Geology*, **21**(1), 3-20.

Oosterhout, J., 1993. An Introduction to TCL and TK.

Powell, R. & Holland, T. J. B., 1985. An internally consistent thermodynamic dataset with uncertainties and correlations: 1. Methods and a worked example. *Journal of Metamorphic Geology*, **3**(4), 327-342.

Powell, R. & Holland, T. J. B., 1988. An internally consistent dataset with uncertainties and correlations: 3. Applications to geobarometry, worked examples and a computer program. *Journal of Metamorphic Geology*, **6**(2), 173-204.

Powell, R. & Holland, T. J. B., 1999. Relating formulations of the thermodynamics of mineral solid solutions: activity modeling of pyroxenes, amphiboles, and micas. *American Mineralogist*, **84**, 1-14.

Powell, R., Holland, T. J. B. H. & Worley, B., 1998. Calculating phase diagrams involving solid solutions via non-linear equations, with examples using THERMOCALC. *Journal of Metamorphic Geology*, **16**(4), 577-588.

Rosenberg, C. L. & Handy, M. R., 2005. Experimental deformation of partially melted granite revisited: implications for the continental crust. *Journal of Metamorphic Geology*, **23**, 19-28.

Sawyer, E. W., 1996. Melt segregation and magma flow in migmatites: implications for the generation of granite magmas. *Geological Society of America Special Papers*, **315**, 85-94

Sawyer, E. W., 2001. Melt segregation in the continental crust: distribution and movement of melt in anatectic rocks. *Journal of Metamorphic Geology*, **19**, 291-309.

Scaillet, B., Holtz, F. & Pichavant, M., 1998. Phase equilibrium constraints on the viscosity of silicic magmas: 1. Volcanic-plutonic comparison. *Journal of Geophysical Research: Solid Earth (1978–2012)*, **103**(B11), 27257-27266.

- Steele, G. L., & Sussman, G. J., 1975. Scheme: An interpreter for the extended lambda calculus. *Artificial Intelligence Lab Memo*, **349**.
- Stevens, G., Villaros, A. & Moyen, J. F., 2007. Selective peritectic garnet entrainment as the origin of geochemical diversity in S-type granites. *Geology*, **35**(1), 9-12.
- Tajčmanová, L., Connolly, J. A. D. & Cesare, B., 2009. A thermodynamic model for titanium and ferric iron solution in biotite. *Journal of Metamorphic Geology*, **27**, 153-165.
- Taylor, J. & Stevens, G., 2010. Selective entrainment of peritectic garnet into S-type granitic magmas: evidence from Archaean mid-crustal anatectites. *Lithos*, **120**(3), 277-292.
- Villaros, A., Stevens, G., Moyen, J. F. & Buick, I. S., 2009. The trace element compositions of S-type granites: evidence for disequilibrium melting and accessory phase entrainment in the source. *Contributions to Mineralogy and Petrology*, **158**, 543-561.
- White, R. W. & Powell, R., 2002. Melt loss and the preservation of granulite facies mineral assemblages. *Journal of Metamorphic Geology*, **20**, 621-632.
- White, R. W. & Powell, R., 2010. Retrograde melt–residue interaction and the formation of near-anhydrous leucosomes in migmatites. *Journal of Metamorphic Geology*, **28**, 579-597.
- White, R. W., Powell, R. & Holland, T. J. B., 2001. Calculation of partial melting equilibria in the system $\text{Na}_2\text{O}-\text{CaO}-\text{K}_2\text{O}-\text{FeO}-\text{MgO}-\text{Al}_2\text{O}_3-\text{SiO}_2-\text{H}_2\text{O}$ (NCKFMASH). *Journal of Metamorphic Geology*, **19**, 139-153.
- White, R. W., Powell, R. & Holland, T. J. B., 2007. Progress relating to calculation of partial melting equilibria for metapelites. *Journal of Metamorphic Geology*, **25**, 511-527.
- White, R. W., Powell, R., Holland, T. J. B. & Worley, B. A., 2000. The effect of TiO_2 and Fe_2O_3 on metapelitic assemblages at greenschist and amphibolite facies conditions:

mineral equilibria calculations in the system K_2O - FeO - MgO - Al_2O_3 - SiO_2 - H_2O - TiO_2 - Fe_2O_3 . *Journal of Metamorphic Geology*, **18**, 497-512.

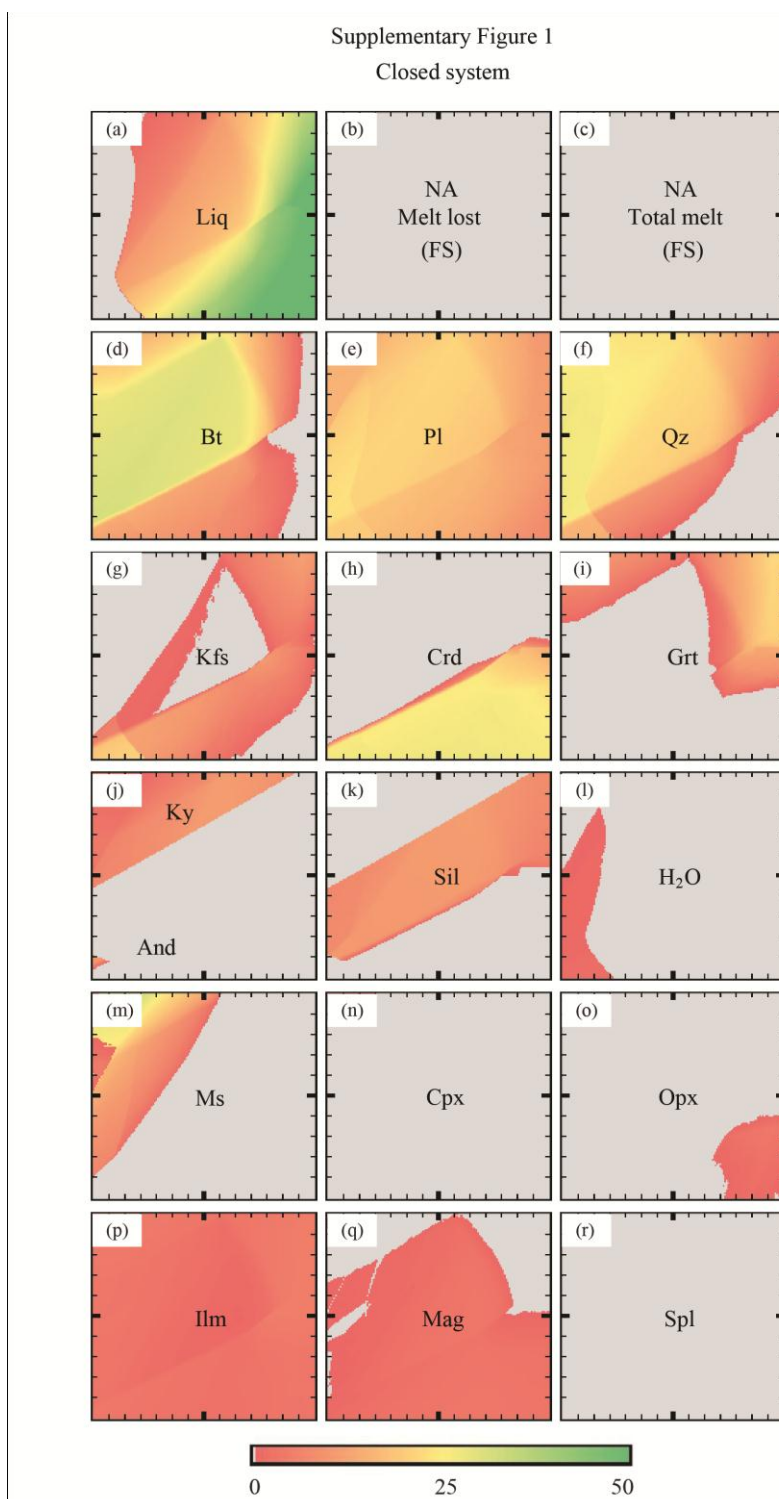
Whitney, D. L. & Evans, B. W., 2010. Abbreviations for names of rock-forming minerals. *American Mineralogist*, **95**, 185-187.

Wood, B. J., Nell, J., & Woodland, A. B., 1991. Macroscopic and microscopic thermodynamic properties of oxides. In *Reviews in Mineralogy and Geochemistry* (1 ed., Vol. **25**, pp. 265-302).

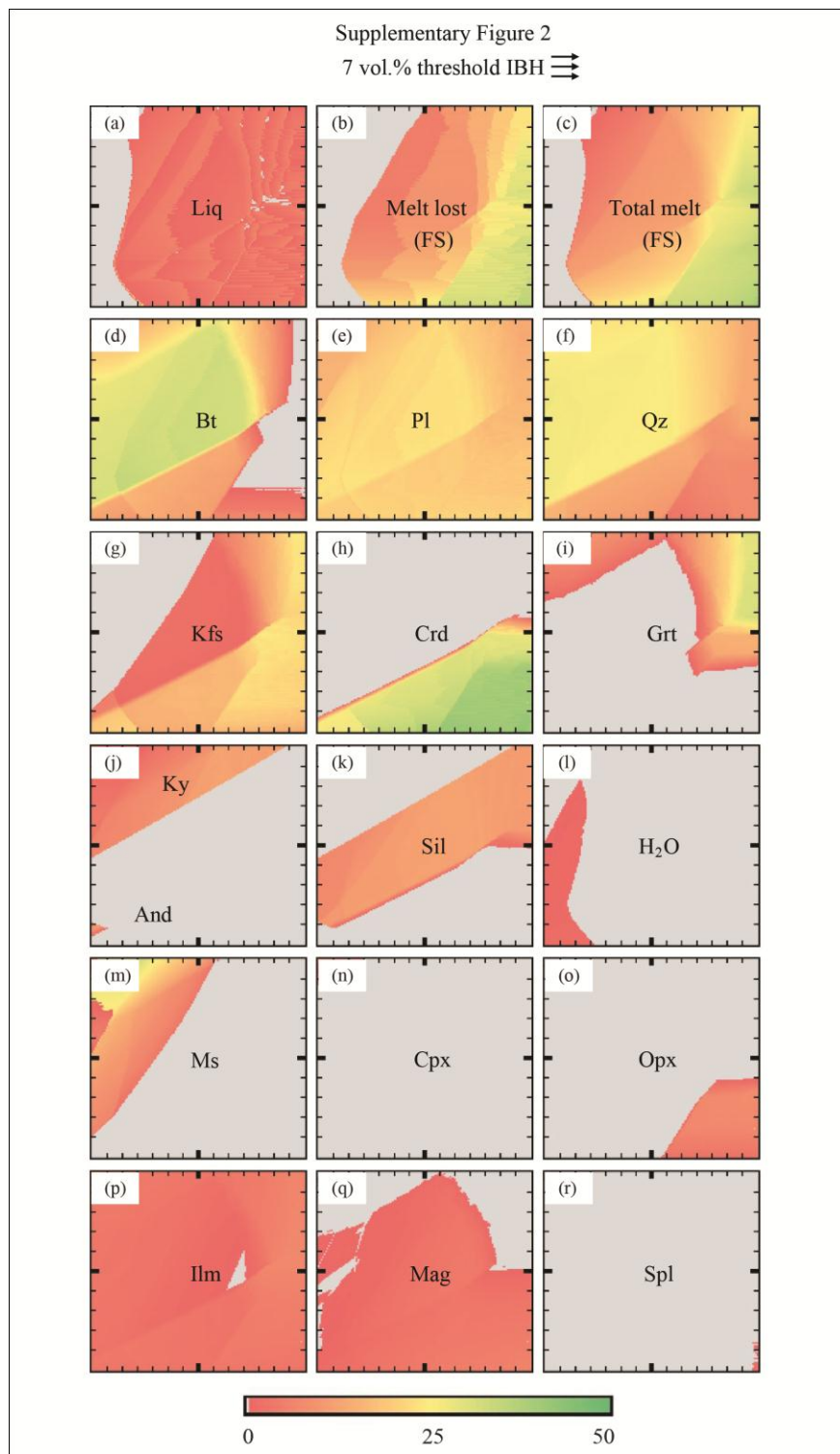
Yakymchuk, C. & Brown, M., 2014. Consequences of open-system melting in tectonics. *Journal of the Geological Society*, **171**, 21-40.

Zuluaga, C. A., Stowell, H. H. & Tinkham, D. K., 2005. The effect of zoned garnet on metapelite pseudosection topology and calculated metamorphic PT paths. *American Mineralogist*, **90**(10),1619-1628

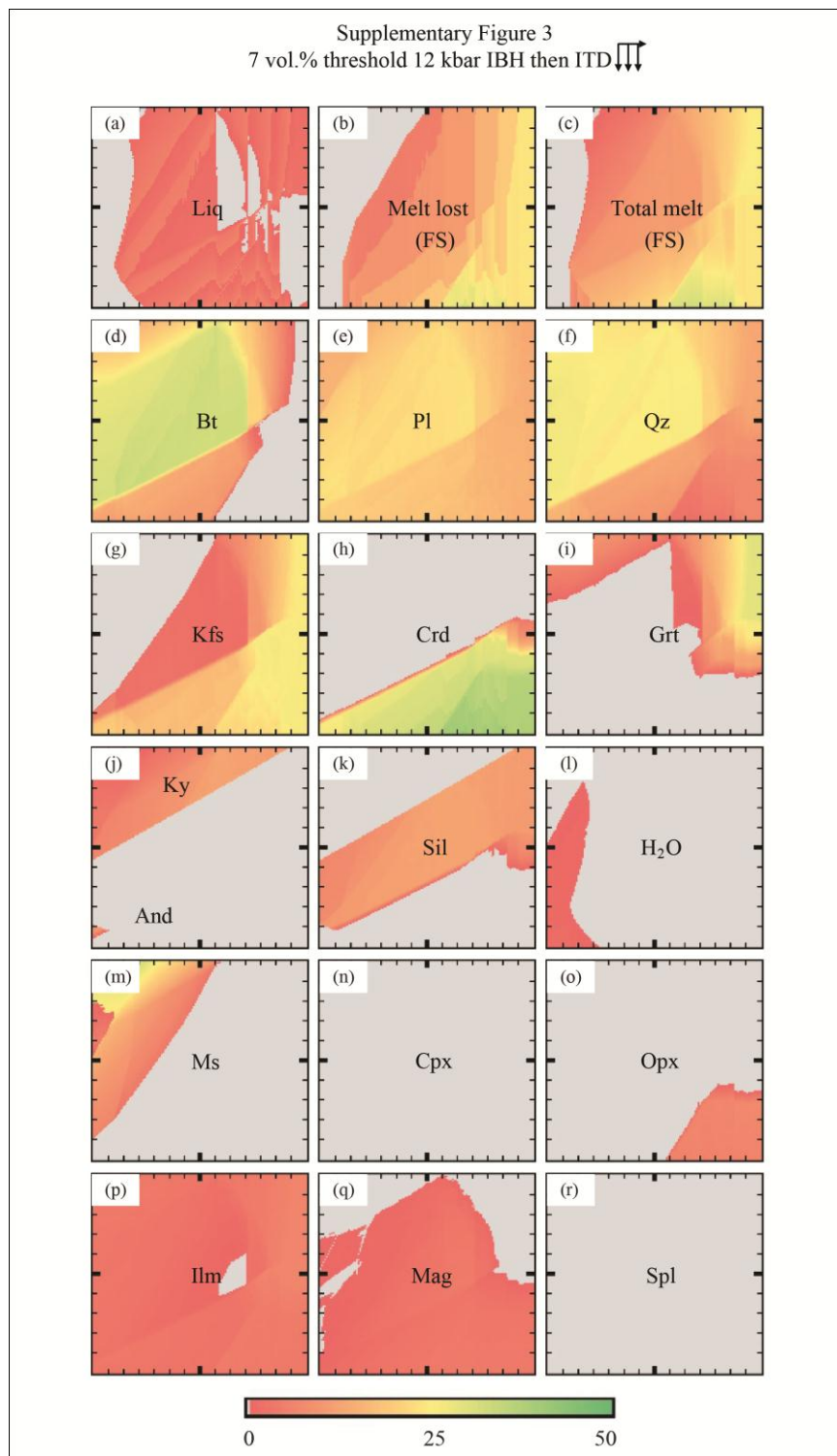
SUPPLEMENTARY FIGURES



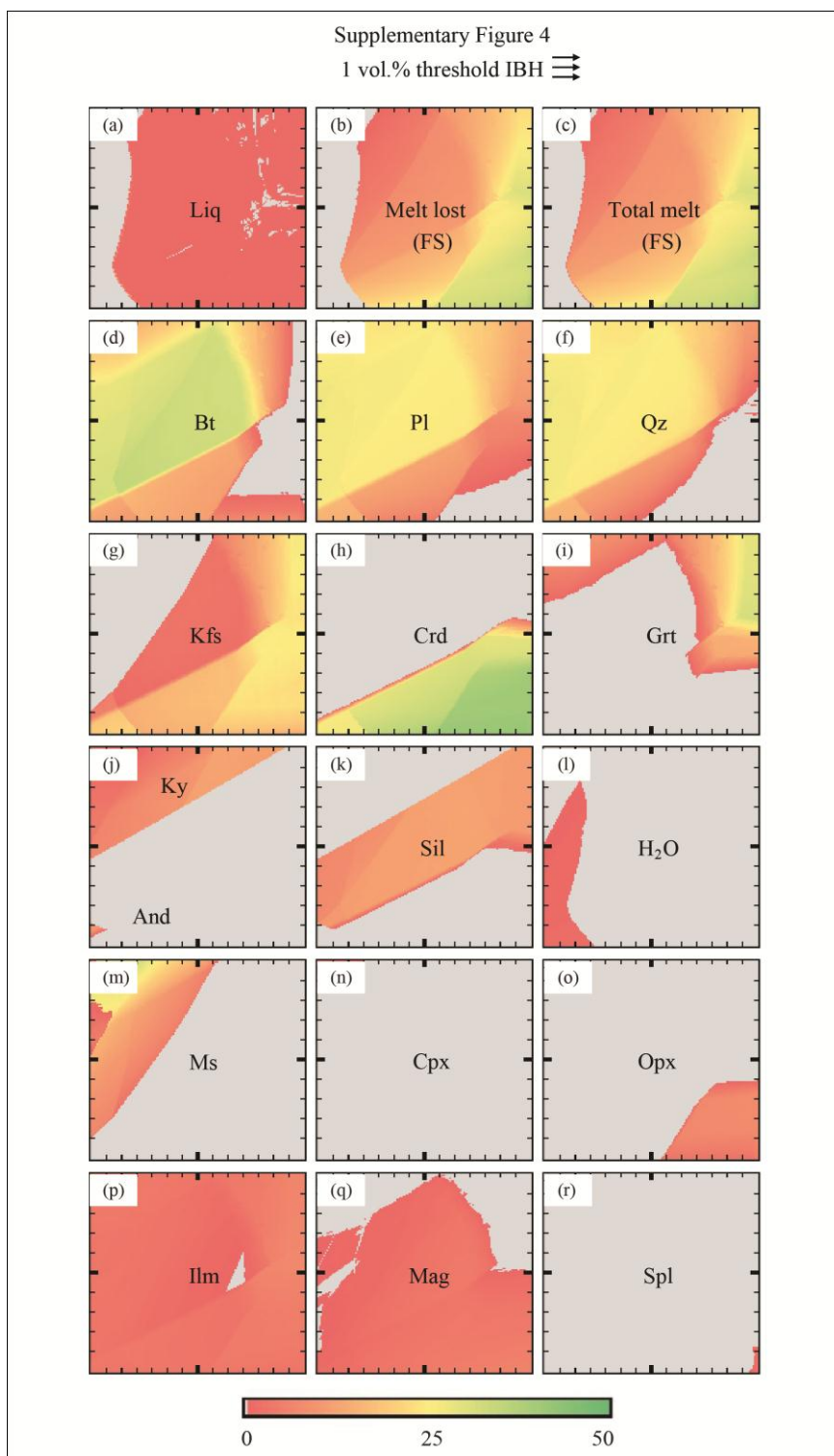
Supplementary Figure 1 - Contour plots for P - T modes in the closed system. (a) melt in the reactive subsystem (b) cumulative (along each path) melt extracted from the reactive subsystem; (c) cumulative (along each path) total melt in the full system (FS); (d-r) phase abundances in the reactive subsystem. Abundances are given as wt.% scaled from 0 wt.%(red) through 25 wt.%(yellow) to 50 wt.% (green) with null values given in grey. Weight percentages for (b & c) are calculated relative to the full system (FS) whereas weight percentages for (a & d-r) are calculated relative the reactive subsystem (RS).



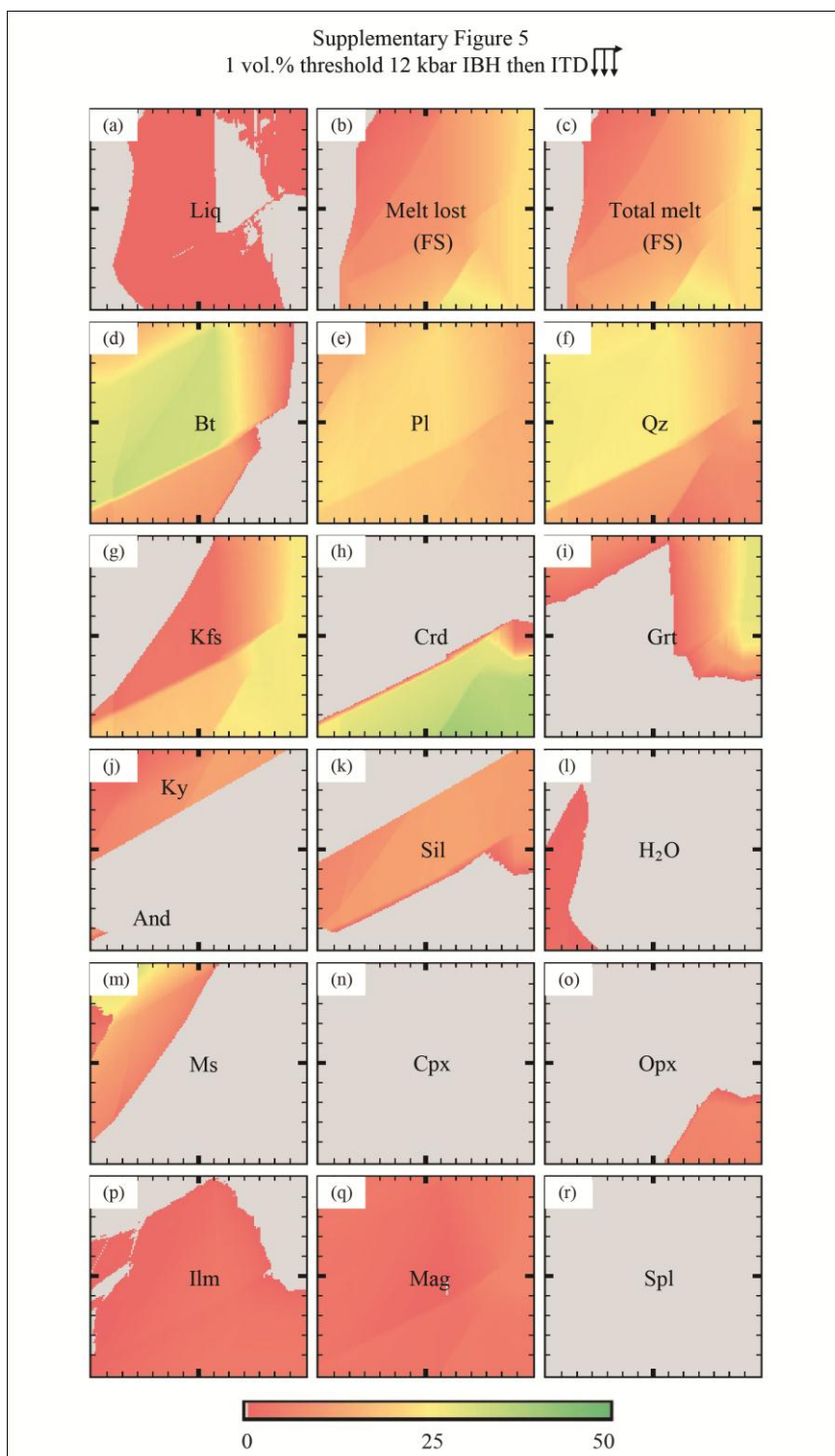
Supplementary Figure 2 - Contour plots for *path-dependent P-T* modes in the 7 vol.% threshold isobaric heating (IBH) system. (a) melt in the reactive subsystem (b) cumulative (along each path) melt extracted from the reactive subsystem; (c) cumulative (along each path) total melt in the full system (FS); (d-r) phase abundances in the reactive subsystem. Abundances are given as wt.% scaled from 0 wt.%(red) through 25 wt.%(yellow) to 50 wt.% (green) with null values given in grey. Weight percentages for (b & c) are calculated relative to the full system (FS) whereas weight percentages for (a & d-r) are calculated relative the reactive subsystem (RS).



Supplementary Figure 3 - Contour plots for *path-dependent P-T* modes in the 7 vol.% 12kbar isobaric heating followed by isothermal decompression system (ITD). (a) melt in the reactive subsystem (b) cumulative (along each path) melt extracted from the reactive subsystem; (c) cumulative (along each path) total melt in the full system (FS); (d-r) phase abundances in the reactive subsystem. Abundances are given as wt.% scaled from 0 wt.%(red) through 25 wt.%(yellow) to 50 wt.% (green) with null values given in grey. Weight percentages for (b & c) are calculated relative to the full system (FS) whereas weight percentages for (a & d-r) are calculated relative the reactive subsystem (RS).



Supplementary Figure 4 - Contour plots for *path-dependent P-T* modes in the 1 vol.% threshold isobaric heating (IBH) system. (a) melt in the reactive subsystem (b) cumulative (along each path) melt extracted from the reactive subsystem; (c) cumulative (along each path) total melt in the full system (FS); (d-r) phase abundances in the reactive subsystem. Abundances are given as wt.% scaled from 0 wt.%(red) through 25 wt.%(yellow) to 50 wt.% (green) with null values given in grey. Weight percentages for (b & c) are calculated relative to the full system (FS) whereas weight percentages for (a & d-r) are calculated relative the reactive subsystem (RS).



Supplementary Figure 5 - Contour plots for *path-dependent P-T* modes in the 1 vol.% 12kbar isobaric heating followed by isothermal decompression system (ITD). (a) melt in the reactive subsystem (b) cumulative (along each path) melt extracted from the reactive subsystem; (c) cumulative (along each path) total melt in the full system (FS); (d-r) phase abundances in the reactive subsystem. Abundances are given as wt.% scaled from 0 wt.%(red) through 25 wt.%(yellow) to 50 wt.% (green) with null values given in grey. Weight percentages for (b & c) are calculated relative to the full system (FS) whereas weight percentages for (a & d-r) are calculated relative the reactive subsystem (RS).

CHAPTER 3

ADDENDA

ADDENDUM A: Electronic copy of Rcrust software

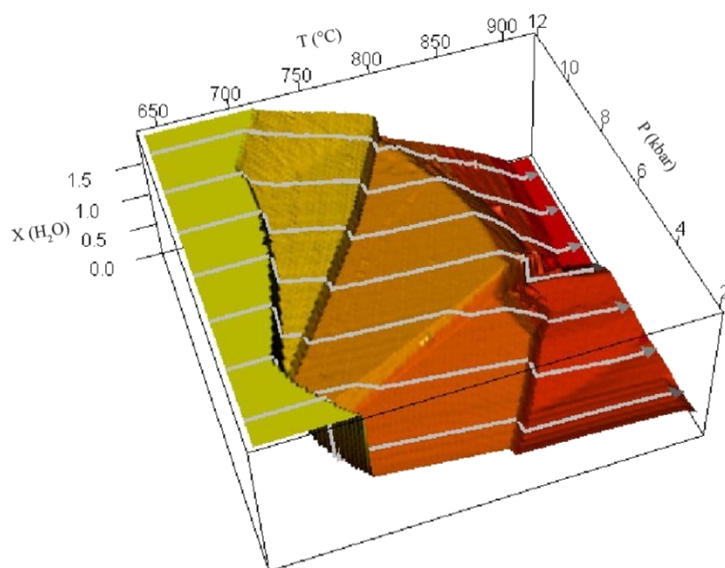
Included within the thesis files for evaluation is the Rcrust program and manual developed as part of the thesis by M.J. Mayne from a starting software by J.-F. Moyen. For a summary of contributions refer to the CONTRIBUTIONS OF THE AUTHORS chapter.

ADDENDUM B: Manual for Rcrust software



Phase stabilities with Path dependence

MJ Mayne, JF Moyen 16 November 2015



Getting started

Installation	2
Example1 – Simple.....	3
Example2 – Phase extraction.....	6
Example3 – Phase addition.....	8

Reference manual

Concept.....	10
Rcrust file management	12
Input parameters	13
Additional settings.....	19
Useful functions.....	24
Development.....	25
Troubleshooting.....	26

GETTING STARTED

Installation

Rcrust was developed using version 3.1.2 (2014-10-31) of R. Copyright © 2014 the R Foundation for Statistical Computing. To install Rcrust perform the following steps:

1. Copy the Rcrust folder to a location of your choice (preferably a root directory for example C:\ or D:\ as this directory should remain unmoved to maintain the program's integrity). The result should be similar to the picture below with all the Rcrust files contained in single directory for example D:\\Rcrust\

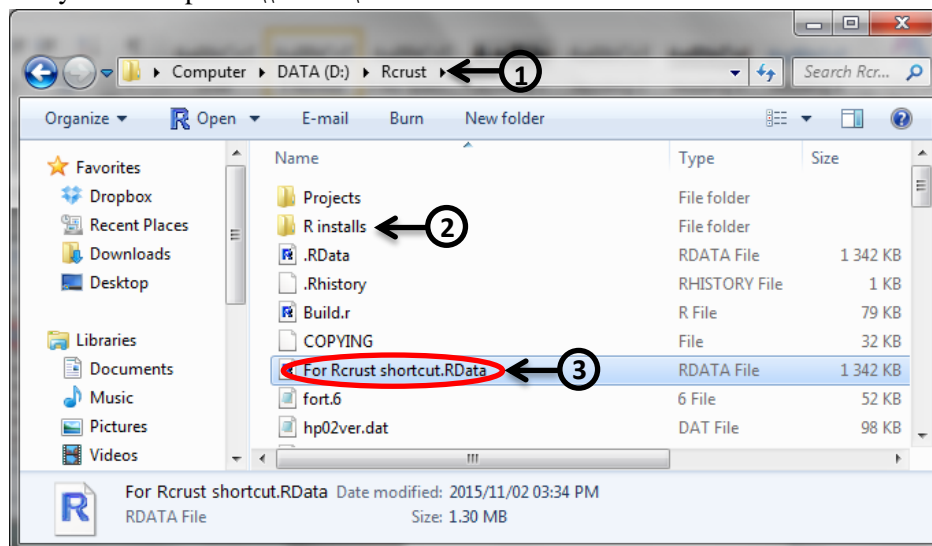
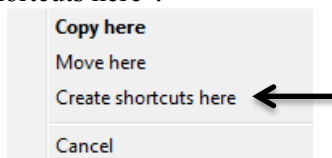


Figure 1 - Rcrust file structure loaded in the root directory D:\\Rcrust\

2. Install a working version of R on your system (at least version 3.1.2).
The latest version of R used in the development of Rcrust is located in the folder “R installs” for your convenience.

*Alternatively newer versions of R (which may not be compatible with Rcrust) can be downloaded from <http://www.r-project.org/> or for windows can be found directly at <http://cran.r-project.org/bin/windows/base/>

3. Right click and drag the “For Rcrust shortcut.RData” file (circled in red above) onto the desktop and choose “create shortcuts here”.



4. Rename this file to “Rcrust”. Double clicking this shortcut will automatically open Rcrust. Each new project will be automatically saved in the “Projects” folder along with its associated inputs and outputs. To load a previously saved project simply double click the “xxx.RData” file in the associated project folder or open Rcrust from the desktop shortcut and load the project via the Rcrust GUI.

Examples

Below are 3 example simulations to get you started using Rcrust. Explanations are between steps.

Example1 – Simple

Follow the bold numbered steps

To begin the first example open Rcrust via the desktop shortcut.

1. Double click the Rcrust desktop shortcut

This will launch the R console and an empty Rcrust Graphical User Interface (GUI). The “**Working File**” (circled in red) shows you which file is currently being worked on and the “**Working Directory**” (circled in green) shows you where the projects folder is located. The Rcrust toolbar contains buttons for file management.

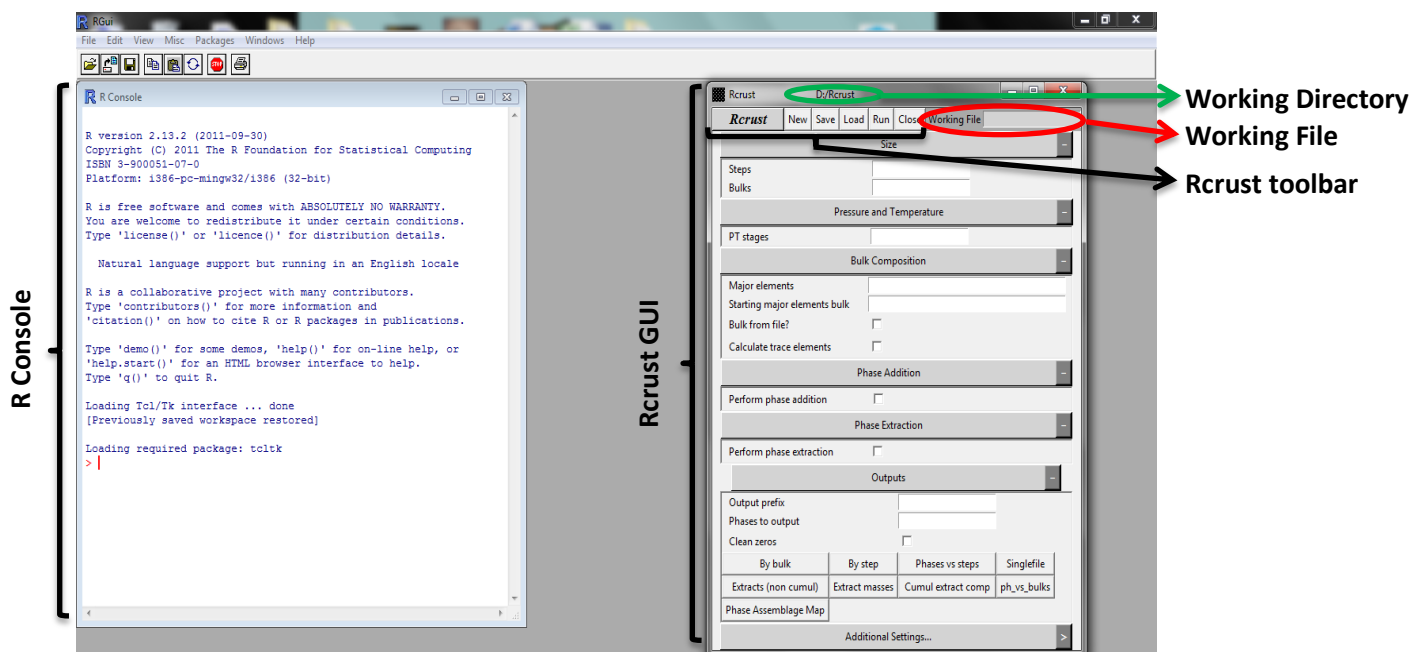


Figure 2 - R Console (left) and Rcrust GUI (right) showing positions of Working Directory (green), Working File (red) and Rcrust toolbar (black).

Note: If components of the Rcrust GUI are off the screen simply collapse some of the tabs to shrink the interface.

2. Type “Example1” into the text box on the right of Working File and press [enter]

The data previously saved in the “Example1” file is now loaded into R and previously saved input parameters are loaded into the Rcrust GUI. To ensure that we do not overwrite any data lets rename the Working File.

3. Rename Example1 by typing “Example_simple” into the Working File textbox then click the Save button from the Rcrust toolbar

This will save the current Rcrust GUI inputs into a new file named “Example_simple”.

Understanding the Inputs:

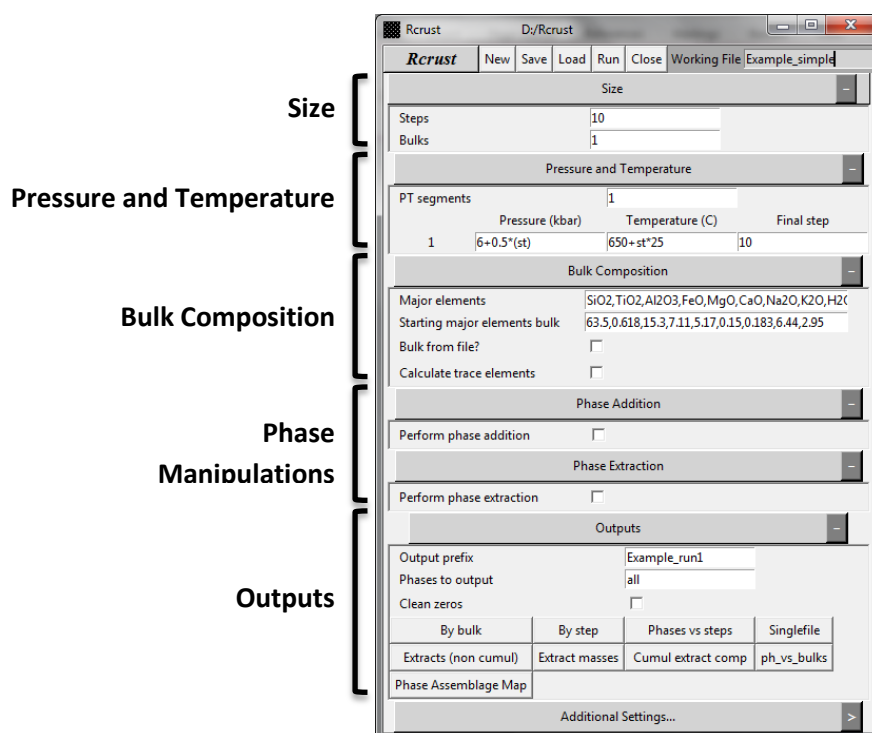


Figure 3 - Rcrust GUI with Example1 (Example_simple) parameters loaded. The parameters are grouped into collapsible tabs. Additional settings can be found by toggling the “Additional Settings...” button.

This example calculates the phases encountered along a simple P-T path. Input parameters are grouped into collapsible tabs. In the “**Size**” tab we see that this P-T path consists of 10 steps (**Steps** = 10) and is calculated for just 1 bulk composition (**Bulks** = 1).

P-T paths are created in the **Pressure and Temperature** tab by multiple line segments with each unique gradient having its own P-T segment. These segments can be defined as individual points or as functions of the step and bulk using “**st**” and “**blk**” variables respectively. **Temperature** is defined in degrees Celsius and **Pressure** in kbar. For this simple P-T path we have only one gradient (**PT segments** = 1) with **Temperature** incremented by 25 degrees Celsius for each step and **Pressure** by 0.5 kbar. The gradient is maintained for the entire path so the PT segments final step equals the final step of the calculation (**Final step** = 10).

In the **Bulk Composition** tab we define the **Major elements** to be modelled and all the starting bulk compositions. In this case **Bulks** = 1 so we define only one starting composition.

Phase Manipulations can alter the bulk composition of the reactive subsystem and outputs can be chosen from the **Outputs** tab. The underlying phase stability calculation settings and solution models chosen are set in “**Additional Settings**” we will return to these settings in future examples.

Once you have a basic understanding of the chosen input parameters let’s launch our first Rcrust calculation.

4. Click the Run button from the Rcrust toolbar

This will launch the calculation procedure into the R console. To see the live calculation progress turn off output buffering by going to the R Console and clicking Misc>Buffered output

5. Go to the R console and Press Misc>Buffered output to uncheck buffering

The R console should now have a few lines of text in it (like the figure below): first describing the license agreement, some advice on how to get help in R and then a track of the initialization sequence. If everything went to plan the final lines in the R console will confirm that the initialization of our

chosen parameters was successful. If your simulation successfully initialized like the one below then we are ready to start the calculation. If your console failed to initialize the program try reloading the original “Example1” file by closing Rcrust then starting from step 1 again, if problems persist try reinstalling Rcrust or report the problem to the developers.

```

RGui
File Edit View Misc Packages Windows Help

R Console

[Previously saved workspace restored]

Loading required package: toltk
Preparing the data matrices...
1 different compositions with
10 successive steps
Bulk compositions...
PT conditions...
phase addition conditions...
phase extraction conditions...
Done with data structures preparation !
.....
Initializing bulk composition...
Trace elements not modelled
Constant bulk composition used for majors -- defined in config file
Done with compo matrix preparation !
.....
Creating meemum build file...
Read 5858 items
Created meemum build file as C:/Rcrust/meemum_build.dat
Initializing PT conditions...
Calculating PT conditions from build...
Done with PT conditions !
.....
No phase addition.
Done with phase addition options !
.....
No phase extraction.
Done with phase extraction options !
.....
Done with initiation. Please read the above lines and make sure this is what yo$
> Choose "n" to abort or press [enter] to continue

```

Figure 4 - The Rcrust calculation is launched into the R Console which tracks the calculation progress and is currently waiting for a response to continue or abort.

6. Press [enter] in the R console to continue

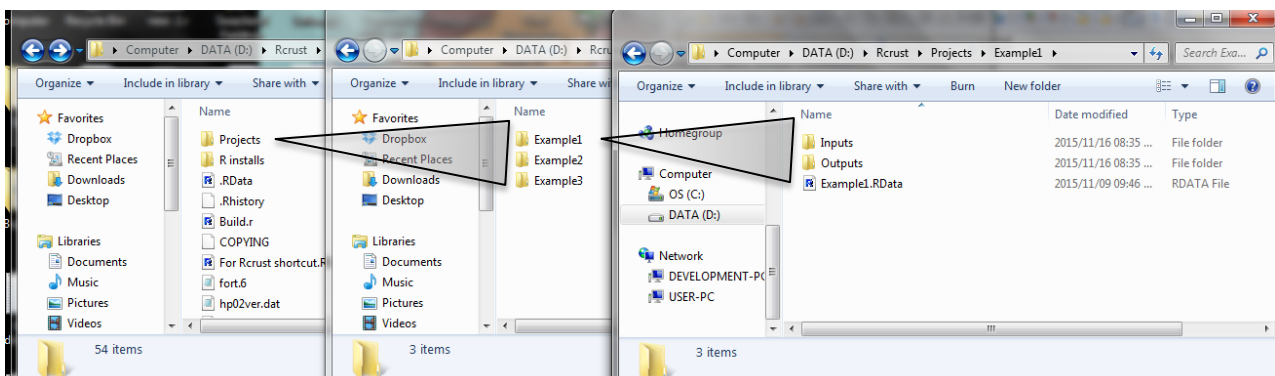
The calculation will run for 10 steps after which you can directly interact with the data in the R console by pressing [enter] in the R console or choose appropriate automated outputs from the Outputs tab. Before we continue let's save our progress as the calculation results are stored in R but they have not yet been saved to our **Working File**.

7. Click Save from the Rcrust toolbar

Now we can write outputs, plot graphs and interrogate data in R knowing that we can always return to our data by reloading our simulation. Let's plot a graph illustrating the phase proportion of our example simulation.

8. Click the Phases vs steps button from the Outputs tab

When outputs are selected .txt files are automatically written to Workingfile folder located in the projects directory. By default the Workingfile folder contains folders for Inputs and for Outputs.



Below is a graph plotted automatically in R by pressing the “Phases vs steps” button.

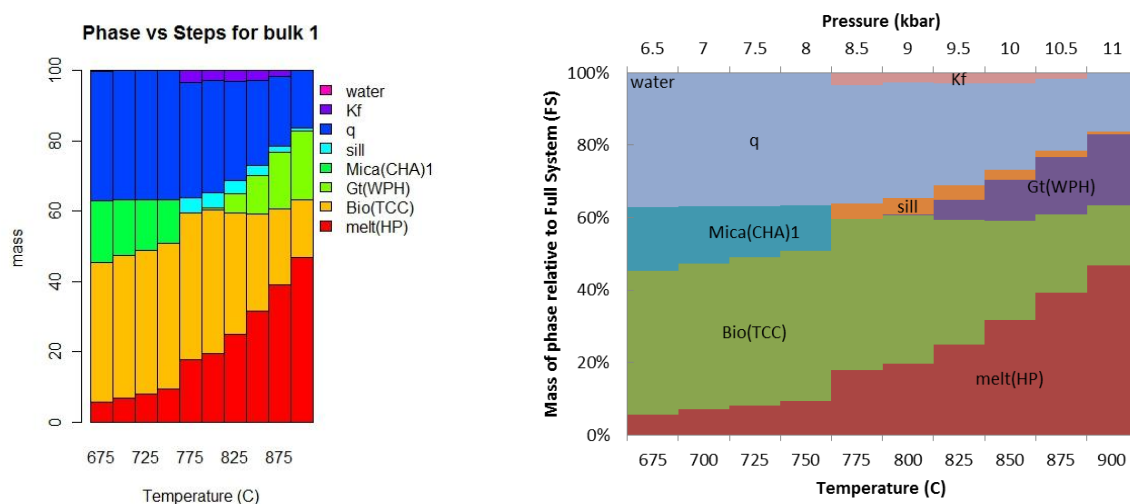


Figure 5 - The Rcrust (left) and excel (right) graphs show the phase proportions of the system during melting of a mica and then biotite as pressure and temperature increase. Peritectic garnet, sillimanite and alkali-feldspar form but the alkali-feldspar is consumed before 11 kbar and 900°C.

Example2 – Phase extraction

Phase extractions can remove phases from contributing to the effective bulk composition of the reactive subsystem. This can be used to simulate scenarios such as melt loss or fractional crystallization.

Let’s perform a melt extraction on the simulation from Example1.

- 1. If continuing from Example1 then skip this step, If starting from scratch load the results of Example1 by opening Rcrust and typing “Example1” into Working File then press [enter]**

To ensure that we do not overwrite any data lets rename the Working File.

- 2. Rename the file by typing “Example_extract” into Working File then click the Save button from the Rcrust toolbar**

This will save the current Rcrust GUI inputs into a new file named “Example_extract”.

- 3. Check the “Perform phase extraction” box in the Phase Extraction tab**

Multiple phases can be set for extraction by separating them with a comma in the Phases entry box but for now let’s just extract melt (we are using the melt(HP) model by default, this can be changed under “Additional Settings...”).

- 4. Type “melt(HP)” in the Phases entry of the Phase Extraction tab**

Phase extraction definitions can be broken into a number of different stages. For this example let’s extract melt at each point along the length of the P - T path by the same condition thus we only require 1 stage.

- 5. Type “1” in the Stages entry of the Phase Extraction tab and then press [enter]**

A new dialog appears with a number of columns adjusted by the number of phases and the number of rows equivalent to the number of stages. For each phase either a specific amount (in grams) can be extracted or a percentage of what is present. Let’s extract 80% of the phase present.

- 6. Type “80%” in the dialog box under melt(HP) for stage 1**

The stages can be divided by conditions or by step numbers, since we want to extract at all points along the P - T path and this consists of 10 steps in our simulation, 10 will be our Final Step.

7. Type “10” in the dialog box under Condition/Final Step for stage 1

We have now set up phase extraction to extract 80% of all melt(HP) present at each point along the P-T path. Your Rcrust GUI should match the one below if you have made a mistake you can load these parameters directly by typing “Example2” in Working File and press [enter], then rename the file to Example_extract:

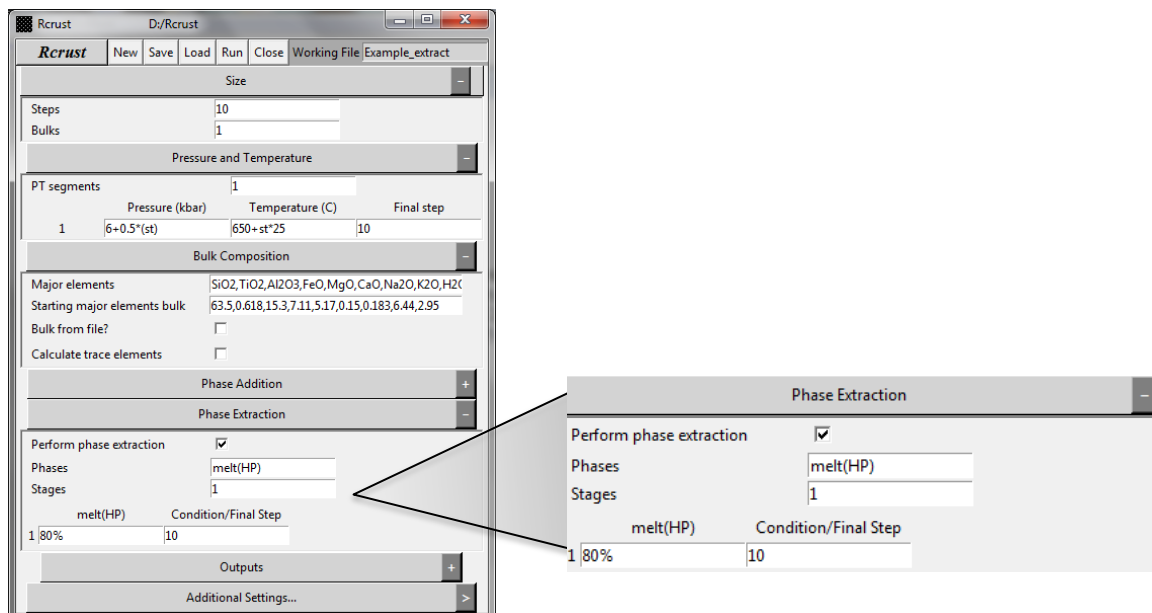


Figure 6 - Rcrust GUI with Example2 (Example_extract) parameters loaded.

Run the calculation and output a phase vs steps graph to view the results. The results of the phase extraction are plotted below.

8. Follow steps 4 to 8 from Example 1

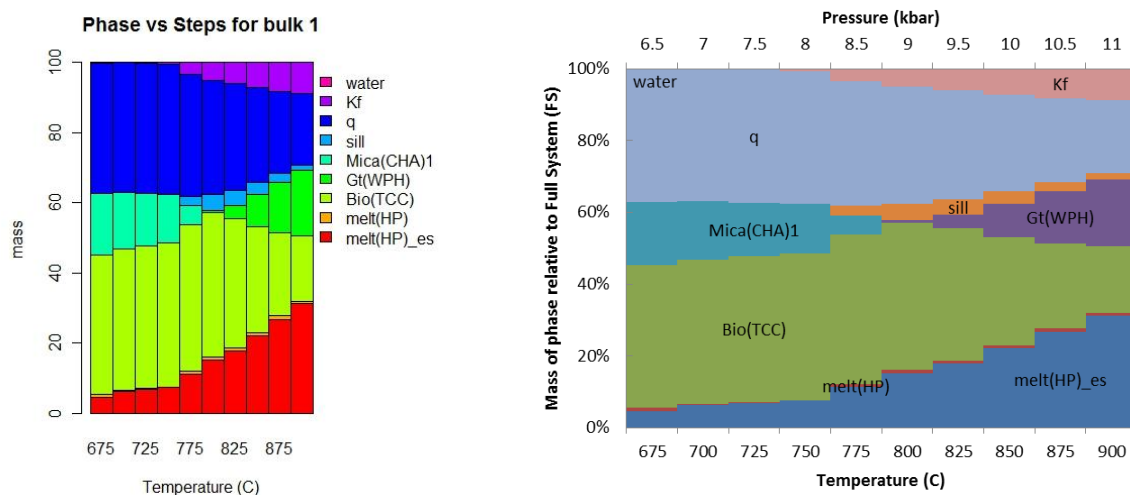


Figure 7 - The Rcrust (left) and excel (right) graphs show the phase proportions of the system during melting of a mica and then biotite as pressure and temperature increase. 80% of melt present at each step is extracted and stored in the extract subsystem as melt(HP)_es. The extraction of melt reduces the total mass of melt that forms and allows peritectic alkali-feldspar to persist to higher temperatures and pressures.

Notice here that 80% of melt that forms is extracted at each step but this does not mandate that the reactive subsystem has 20% melt at the end of each step. The reactive subsystem is thermodynamically re-equilibrated at the end of each step to its new effective bulk composition so this may change the phase proportions. Extracts are added cumulatively at each step yielding a total

extracted mass with a weighted average composition. The details of each individual extract are available through the Extracts (non cumul) button in Output Mode or by typing the R variable “extract” into the console and pressing enter. Extracts are not thermodynamically re-equilibrated to the reactive subsystem or the P - T conditions and can be compilations of multiple phases in solid solution.

Example3 – Phase addition

Phase additions can include new phases in the effective bulk composition of the reactive subsystem. This can be used to simulate scenarios such as dissolution or contamination.

Let’s add a phase addition to the simulation from Example2. Let’s arbitrarily assume (for illustration purposes) that water is added as 1 gram per step from step 8 onwards on our P-T path.

- 1. If continuing from Example2 then skip this step, If starting from scratch load the results of Example2 by opening Rcrust and typing “Example2” into Working File then press [enter]**

To ensure that we do not overwrite any data lets rename the Working File.

- 2. Rename the file by typing “Example_add” into Working File then click the Save button from the Rcrust toolbar**

This will save the current Rcrust GUI inputs into a new file named “Example_add”.

- 3. Check the “Perform phase addition” box in the Phase Addition tab**

Multiple phases can be set for addition by separating them with a comma in the Phases entry box but for now let’s just add water.

- 4. Type “water” in the Phases entry of the Phase Addition tab**

Phase addition definitions can be broken into a number of different stages. For this example let’s add water from step 8 onwards. This requires 2 stages: stage 1 = no water addition from steps 1 to 7; stage 2 = 1g water addition per step from steps 8 to 10 (the end).

- 5. Type “2” in the Stages entry of the Phase Addition tab and then press [enter]**

A new dialog appears to contain phase compositions and a table with the number of columns adjusted by the number of phases and the number of rows equivalent to the number of stages. The composition must be defined as comma separated values in the order of the Major Elements defined in the Bulk composition tab. For our example this is SiO₂,TiO₂,Al₂O₃,FeO,MgO,CaO,Na₂O,K₂O,H₂O.

- 6. Type “0,0,0,0,0,0,0,100” in the water composition dialog box**

For each phase an amount in grams relative to the full system mass (100g by default) must be specified for addition. We’ll add 1g in steps 8,9 and 10 respectively.

- 7. Type “0” in the dialog box under water for stage 1 and Type “1” in the dialog box under water for stage 2**

As stages cannot overlap and must cover the entire P-T path only the Final step is required for each stage with subsequent stages assumed to begin from 1 step after the end of the previous.

- 8. Type “7” in the dialog box under Final Step for stage 1 and Type “10” in the dialog box under Final Step for stage 2. Your inputs should match the figure below.**

We have now set up phase addition to add 1 gram of water per step from step 8 onwards in a system that loses 80% of all melt that forms at each step. Your Rcrust GUI should match the one below, this can be loaded directly if you have made a mistake, by typing “Example3” in Working File and pressing [enter]:

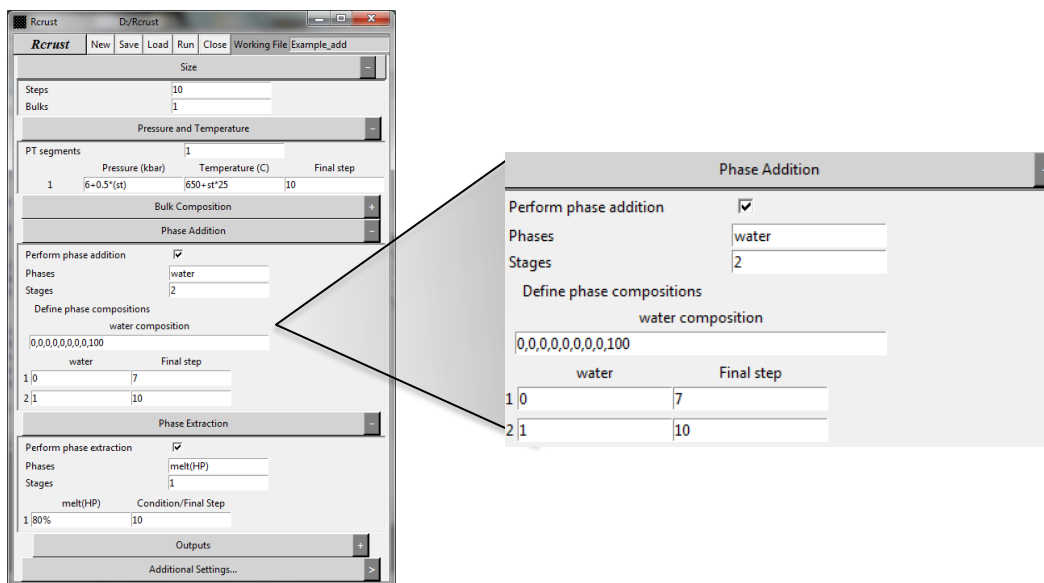


Figure 8 - Rcrust GUI with Example3 (Example_add) parameters loaded.

Run the calculation and output a phase vs steps graph to view the results. The results of the combined phase addition and extraction are plotted below:

9. Follow steps 4 to 8 from Example 1

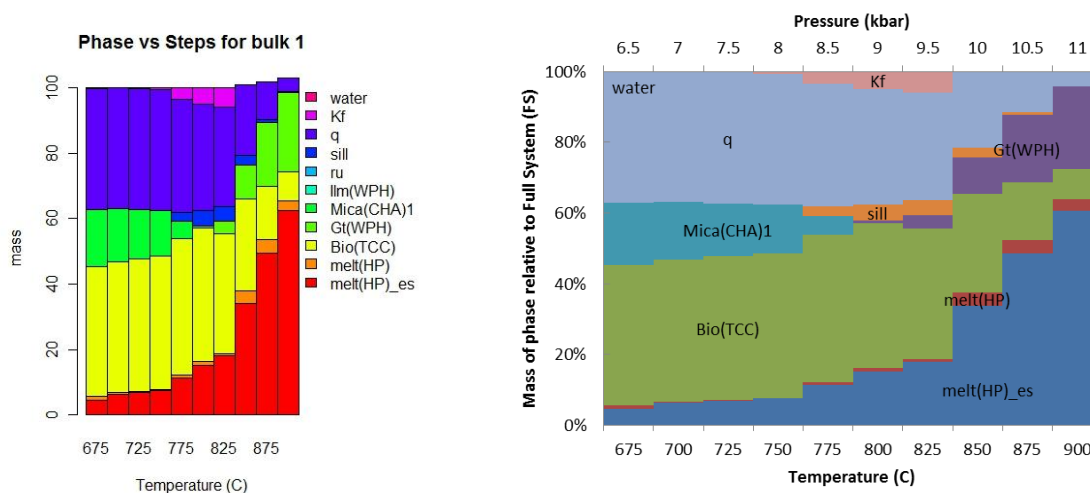


Figure 9 - The Rcrust (left) and excel (right) graphs show the phase proportions of the system during melting of a mica and then biotite as pressure and temperature increase. 1g of water is added in each of steps 8, 9 and 10. Peritectic garnet and alkali-feldspar form but with the addition of water the system produces more melt consuming the alkali-feldspar before 10 kbar and 850°C.

Notice here that we are plotting the mass relative to a starting reactive system with total mass of 100g, thus when water is added the total mass of the full system exceeds 100g. To accurately compare the amount of melt in the full system the values are normalised to 100 in the excel output. Alternatively the starting total mass of the reactive system can be adjusted in meemum.model.r (e.g. if you wish to isolate all of a select phase from the system and reincorporate it back into the reactive system incrementally).

REFERENCE MANUAL

Concept

Rcrust is an R program aimed at modelling with path dependence. The program functions by calculating a number of points in P-T-X space where a bulk composition is passed between points. This creates path dependence as points within the path rely on the outcomes of previous points for their calculation. The bulk composition can be altered at each point by phase manipulations consisting of phase additions and/or phase extractions.

Rcrust manages calculations by splitting the full thermodynamic system (FS) into 3 subsystems: The reactive subsystem (RS) which contains the phases in thermodynamic equilibrium; The addition subsystem (AS) where phases are waiting to be added to the reactive subsystem; and the extract subsystem (ES) where phases extracted from the reactive subsystem are stored. The reactive subsystem is in thermodynamic equilibrium with the P-T-X conditions of each point and is re-equilibrated after each P-T-X change. The addition and extract subsystems are in thermodynamic isolation from other subsystems and from the P-T-X conditions of each point.

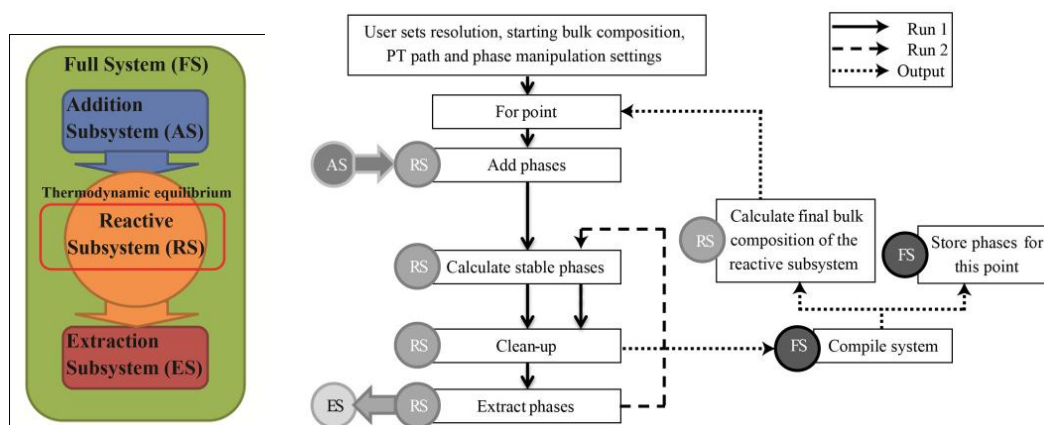


Figure 10 - Relationships between systems (left) and flow chart (right) illustrating the Rcrust program structure for a single path. The user inputs the calculation's resolution, starting bulk composition, P-T path and phase manipulation settings. Each step in a path consists of two runs and an output. The first run is shown in a solid line, the second run in a dashed line and the outputs in a dotted line. Circles show the system or subsystem involved in each step as AS (addition subsystem), ES (extract subsystem), FS (full system) or RS (reactive subsystem). Arrows show interactions between systems.

Parameters for calculations are accessible to the user via the Rcrust Graphical User Interface (GUI). This GUI writes data to a text file which is then input to the program thus allowing the user to edit the file 'behind' the GUI as well as save inputs for re-use. The code files are extensively commented, and described in this document. The calculations routines are defined in several files, written in a modular way that should allow easy addition of features if required. For example the Phase Extraction routine has been modified to suit the needs of magma extraction where additional capabilities allow melt extraction to leave a set melt retention amount behind.

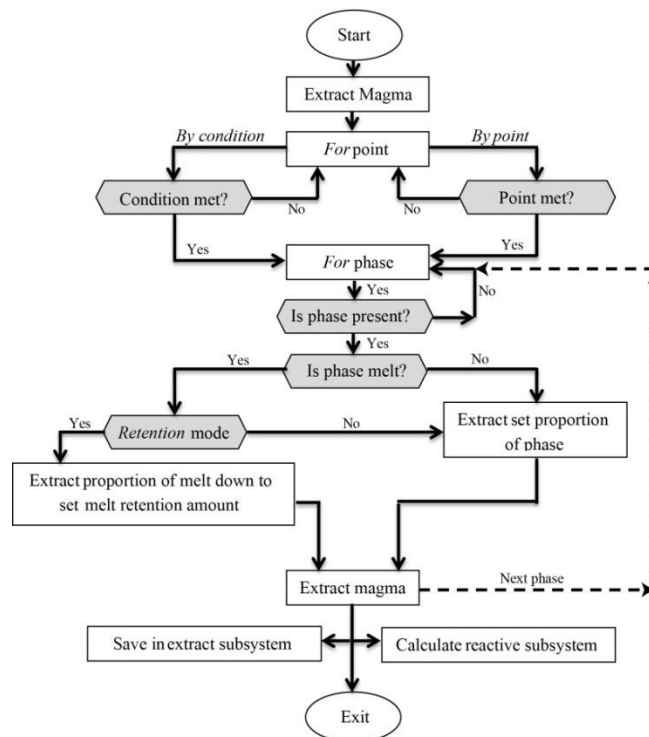


Figure 11 - Flow chart of the magma extraction routine. Grey hexagon shaped boxes are decision points. Coding variables are in italics. The for phase loop (dotted line) is repeated until each phase tagged for extraction has been considered. If Retention mode is active melt is considered last so that other phases extracted are accounted for in its calculation.

Rcrust results should be easily loaded into GCDkit and examined from there.

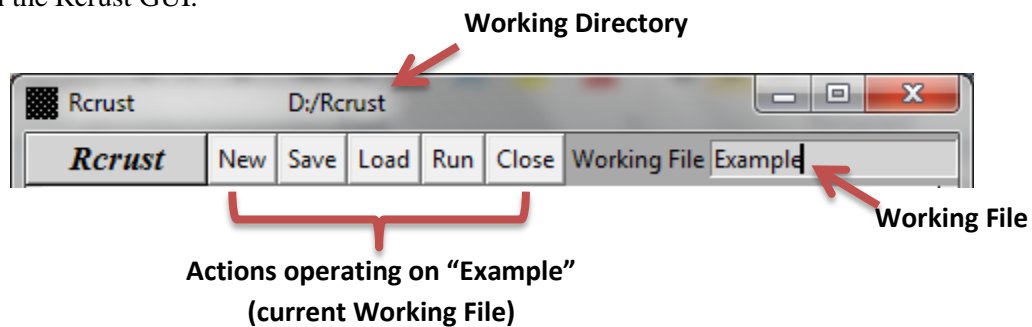
It is important to remember a few things:

- Rcrust is in development. It is not mature software. It is very unstable at the best of times, and very unforgiving in terms of improperly formatted inputs, etc. When Rcrust fails, it will try to generate some human-readable error messages: read them! It may well give you hints at things you can correct in your inputs.
- Most of the errors you will see are related to incorrect input (files with incorrect number of lines etc.); or to exotic phases being produced by meemum.

Rcrust calls Perple_X itself or a set of binary files containing the thermodynamic equations thus relying on published databases (Holland and Powell typically). The output will never be better than the underlying thermodynamic model. Since we focus on melting, we are tied to the capacities (and limitations) of the melt models. For instance melt(HP) is known to be totally unable to predict properly melt—amphibole equilibria....

Rcrust File Management

The topline of the Rcrust GUI hosts a toolbar of file management buttons. User inputs are saved in a text document (Working File). This file is written, read or run in Rcrust by the new, save, load and run buttons in the Rcrust GUI.



New

Creates a new blank project folder and working file under the given working file's name

Save

Calls the writing of a text file that contains all options specified in the Rcrust GUI. The text file is written in the project folder defined by "working file" in a folder called "Inputs". This document is human readable and can be manually altered by users with any text editor. It is good practice to save this file with any completed run as a track of the selected options.

Load

Reads the working file from the inputs folder and places its options in the Rcrust GUI inputs.

Run

Saves the current Rcrust GUI inputs and launches Rcrust according to these parameters. Follow prompts in the R console to calculate the results. Once the results are complete you will be prompted to select outputs. Press enter to reactivate the console and then use the Rcrust GUI Outputs tab to write these results to the "Outputs" folder of the project or load them directly into GCDkit.

Close

Destroys the current window.

Input Parameters

User inputs are listed here in a systematic fashion for clarity. The parameter name is listed first followed by the variable name (to fine out the current value of a parameter type the variable name into the R console and press [enter]). The data type required for the parameter is listed in the second box. The third box contains possible values for the parameter and identifies any default value. Below this is a description as to what the parameter controls.

Variable name	Parameter name	Data type	Possible values
<code>Example Paramater {ex_par}</code>	Integer	0 = closed 1 = open Default = 0	
Example definition for the paramater			Default value
Parameter description			

Size

Specify here the size of the simulation (resolution) you want to calculate: how many bulk compositions and how many steps in the PTX paths.

Size	
Steps	150
Bulks	1

Options

Steps {n_step}	Integer	
Number of steps. Note that the size of other inputs (PT, phase extraction,etc) must conform to this.		

Bulks {n_bulk}	Integer	
Number of bulk compositions. This could correspond to different lithologies, or to different levels in a crust column. Note that the size of other inputs (PT, phase extraction,etc) must conform to this.		

P-T data

This tab defines the pressure and temperature conditions. The conditions are set by a number of ‘*P-T*’ segments which are intervals of *P-T* values that have a unique gradient. These segments can have constant values or can be defined relative to the step “st” or bulk “blk” of the path.

Pressure and Temperature			
PT segments	Pressure (kbar)	Temperature (C)	Final step
1	5+0.05*st	700+2*st	100
2	10	700+2*st	150

PT segments {stage_n}	Integer	
Number of PT segments for which different PT gradients will be set. Note this number must be smaller than or equal to the number of steps. The segments must fill the P-T path exactly with no overlap.		

Pressure (kbar) {press}	Real number, expression	
The pressure in kbar of the system. This can be a constant or an expression using the variables named "st" (step) or "blk" (bulk), real numbers, multiplication(*), division(/), addition(+), subtraction(-) or exponents(^).		

Temperature (C) {temp}	Real number, expression	
The temperature in degree celsius of the system. This can be a constant or an expression using the variables named "st" (step) or "blk" (bulk), real numbers, multiplication(*), division(/), addition(+), subtraction(-) or exponents(^).		

Final Step {t_f}	Integer	
The last step in the specific interval. Each interval begins one step after the previous interval with the first interval starting from step 1. Note the 'Final step' for the last interval must be equal to the total number of steps		

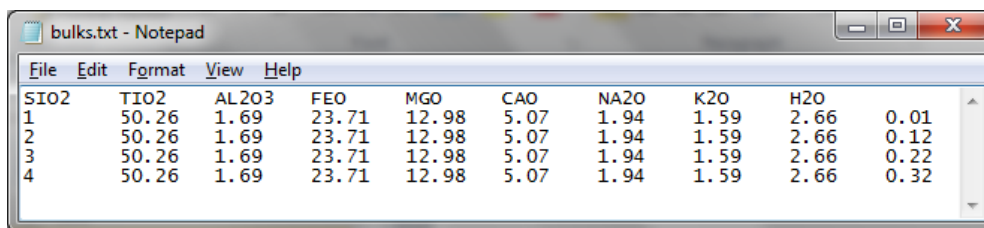
Bulk composition

This section allows the definition of the initial bulk composition (or compositions) of the reactive subsystem.

Major elements {elts}	Character vector (comma separated strings)	
List the elements as oxides separated by commas that are part of the bulk composition (e.g. SiO2,TiO2...).		

Starting major elements bulk {c0_maj_cst}	Numeric vector (comma separated real numbers)	
List the proportion of each major element oxide listed above as comma separated terms for the given bulk (e.g. 65.04,1.79,...). These values are given as wt% by default. The unit for bulk composition definition can be changed in <code>init_meem.r</code> (Perplex options set in <code>init_meem.r</code>)		

Bulk from file {bulk_from_file}	Boolean	T (TRUE) F (FALSE)
Read bulk compositions from a file? The first row of this file must contain the names of the major elements (as below). The first column must contain the number of the bulk and subsequent columns must be tab delimited. The first row must have one less column than the other rows as there must be no name for the bulk number. These values are given as wt% by default. The unit for bulk composition definition can be changed in <code>init_meem.r</code> (Perplex options set in <code>init_meem.r</code>). This file must be located in the Inputs folder of the project and be named "bulks.txt".		



Calculate trace elements {do_traces}	Boolean	T (TRUE) F (FALSE)
Do we want to calculate trace elements? If not, the program will ignore everything related to trace elements. * This functionality is currently in development		

Trace elements {traces}	Character vector (comma separated strings)	
List the trace elements as oxides separated by commas that are part of the bulk composition. When reading the K_D file, Rcrust will drop all elements that are not defined here. * This functionality is currently in development		

Starting trace elements bulk {c0_tr_cst}	Numeric vector (comma separated real numbers)	
List the weight % of each trace element oxide listed above as comma separated terms for the given bulk (e.g. 65.04,1.79,...). * This functionality is currently in development		

Calculate subsolidus traces {do_subsolidus_traces}	Boolean	T (TRUE) F (FALSE)
Should we calculate trace elements partitioning when melt is not present in the system? It's probably not a good idea because you'll have trouble with phases such as Chl, act, ep, etc. If you want to try that you must make sure you have K_D values for all these phases (remember, K_D values are defined relative to melt, even if none is present – this is a pure calculation convention). If you do that, you have the option to use a separate K_D file for sub-solidus cases. * This functionality is currently in development		

Subsolidus kd file {kd_ss_file}	String	
The emplacement (relative to <code>work_dir</code>) of the partition coefficient file used for subsolidus trace partitioning. So far we use only fixed partition coefficients, so we specify only one such file for the whole problem, regardless of PT, bulk, etc. If you want to use the same file for both subsolidus and supersolidus, a simple solution is to enter here <code>kd_ss_file<-kd_file</code> * This functionality is currently in development		

Phase Addition

Set the options for phase addition.

Phase Addition

Perform phase addition

Phases

Stages

Define phase compositions

Plagioclase composition

	Plagioclase	Final step
1	<input type="text" value="0.0107"/>	<input type="text" value="200"/>
2	<input type="text" value="0"/>	<input type="text" value="250"/>

Perform phase addition {ph_add}	Boolean	T (TRUE) F (FALSE)
Do you want to add phases to the bulk at progressive steps?		

Phases {aph}	Character vector (comma separated strings)	
List of the phases to add.		

Stages {ph_add_stage_n}	Integer	
Number of phase addition intervals for which different phase addition conditions will be set. Note this number must be smaller than the total number of steps. The stages must fill the steps exactly with no overlap.		

Define phase compositions {x_comp}	Numeric vector {comma separated real numbers}	
For each phase listed above {aph} a dialog box for that phase's composition will appear. List the weight % of each major element oxide (chosen by Bulk composition/Major Elements) as comma separated real numbers (e.g. 65.04,1.79,...).		

Define phase mass {x.val}	Real number, expression	
For each phase listed above {aph} and each stage set the mass of the phase to add. This can be a constant or an expression in terms of the variable "st" (step). The expression can include any combination of real numbers, multiplication (*), division (/), addition (+), subtraction (-) or exponents (^).		

Final step {ph_add_t_f}	Integer	
The last step in the specific interval. Each interval begins one step after the previous interval with the first interval starting from step 1. Note the 'Final step' for the last interval must be equal to the total number of steps		

Phase Extraction

Set the options for phase extraction.

Phase Extraction		
Perform phase extraction	<input checked="" type="checkbox"/>	
Phases	<input type="text" value="melt(HP)"/>	
Stages	<input type="text" value="1"/>	
	melt(HP)	Condition/Final Step
1	10%	melt(HP),>=,7,vol%

Perform phase extraction {ph_extr}	Boolean	T (TRUE) F (FALSE)
Do you want to extract phases from the bulk at progressive steps?		

Phases {eph}	Character vector (comma separated strings)	
List of the phases to extract.		

Stages {ph_extr_stage_n}	Integer	
Number of phase extraction intervals for which different phase extraction conditions will be set. Note this number must be smaller than the total number of steps. The stages must fill the steps exactly with no overlap.		

Define phase proportions	Real number, expression	[0,1] Expression
For each phase listed above and each stage set the proportion of the phase to extract, proportions can be given as: <ol style="list-style-type: none"> 1. A percentage of what is present (e.g. 10%) *you must include the percentage sign for this 2. A set mass (in g) relative to the full system (100g). The mass can be defined as a constant or an expression in terms of the variable "st" (step). The expression can include any combination of real numbers, multiplication (*), division (/), addition (+), subtraction (-) or exponents (^). 3. Additional phase extraction capabilities exist for melt: by setting Retention mode in meemum_model.r to TRUE, melt is extracted down to a set retention amount (the unit for this amount is set with retention_unit in meemum_model.r). Thus the value given in the phase proportion box now becomes the melt retention amount as opposed to a melt extract amount. 		

Condition/Final step {ph_extr_t f}	Integer, expression	
<ol style="list-style-type: none"> 1. Condition definition: A conditional argument of the form {phase},{condition},{value},{unit} For example to extract phases whenever melt exceeds a 7 vol% threshold you would use the following condition: melt(HP),>=,7,vol% 2. Final step definition: The last step in the specific interval. Each interval begins one step after the previous interval with the first interval starting from step 1. Can be defined as a constant or an expression including any combination of real numbers, multiplication (*), division (/), addition (+), subtraction (-) or exponents (^). Note the 'Final step' for the last interval must be equal to the total number of steps. 		

Outputs

The program creates a list (called crust) with compositions, and the other interesting properties are stored in different variables. The output routine builds a more usable data matrix that can be passed to GCDkit.

The present routine adds to the composition data the (original, step 1) bulk, the P T conditions, the proportion of phases in the small equilibration domains (Bulk, Extract,etc).

Outputs			
Output prefix	Example_run1		
Phases to output	all		
Clean zeros	<input type="checkbox"/>		
By bulk	By step	Phases vs steps	Singlefile
Extracts (non cumul)	Extract masses	Cumul extract comp	ph_vs_bulks
Phase Assemblage Map			

Options

Output prefix {of.prefix}	String	
The output files will be names using the prefix, and a number corresponding to the bulk/step depending on the mode.		
If output_mode=="singlefile", one single file is generated and its name is of_prefix. The file(s) will be written to the outputs folder for the project		

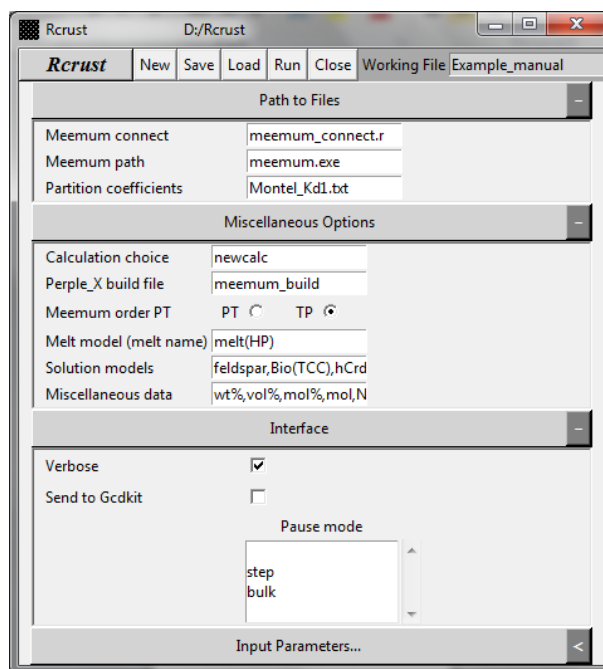
Phases to output {out.ph}	Character vector	
List of the phases to include in the output file(s). The names should match the names of legitimate components of the system (see extraction, above), including the aggregates (Total_extract, etc), e.g. : melt.name, Gt (WPH), Pl, Total_extract, Bulk, Kf.		

Clean zeros {clean.zero}	Boolean	T (TRUE) F (FALSE)
If true, the phases with 0 mass will not be written to the file(s). May or may not be desirable – you may want to keep, for instance, a line for melt at each step even if its amount is 0, perhaps to plot curves of melt production vs. time?		

Output buttons	Selection of output buttons	
Select which outputs to write to file. This file is placed in the Outputs folder of the project.		
<ul style="list-style-type: none"> - By bulk: one file for each bulk, aggregating all the steps; - By step: one file for each step, aggregating all the bulks; - Phases vs steps: only output the mass of each phase as a function of steps - Singlefile: everything in one (presumably large !) file - Extracts (non cumul): The wt% oxide composition of each extract at individual steps - Extract masses: The mass of each phase extracted at each step - Cumul extract comp: The wt% oxide composition of the total extract subsystem at each step - Ph_vs_bulks: only output the mass of each phase as a function of bulks - Phase assemblage map: draws a map of the PTX space assemblages and associated contours 		

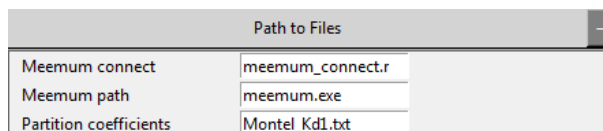
Additional Settings

Further settings can be defined by clicking the right arrow (>) on the Additional Settings tab or by clicking the header itself.



Path to files

Indicate here the location of the files on disk.



Options

Meemum connect {meemum_connect_file}	String	
The emplacement (relative to <code>work_dir</code>) of the meemum connection file, that contains functions “run.meemum” and “read.meemum”.		
Meemum path {meemum.path}	String	
The emplacement (relative to <code>work_dir</code>) of the meemum executable.		
Partition coefficients {kd_file}	String	
The emplacement (relative to <code>work_dir</code>) of the partition coefficient file. So far we use only fixed partition coefficients, so we specify only one such file for the whole problem, regardless of PT, bulk, etc.		

Files

Kd file

A text file that contains partition coefficients for all phases likely to be encountered in the calculations. If a phase is not defined here, but is predicted by meemum, Rcrust will end with an error. Tough luck...

The file must contain one column per element (names corresponding to the names used elsewhere), and one line per mineral (phase). The phase names must be exactly the ones that perple_x will generate (e.g. "Gt (WPH)"), with the following exceptions:

water, for the free water phase;

If the ternary solution "feldspar" is used in perple_x, the code will recognize it and decide whether the feldspar(s) is plagioclase, or K-feldspar. In this case it will replace feldspar by "Pl" and "Kf" respectively (in function cleanup() of the main.r file), and these minerals with these exact names must be present in the Kd file.

As with all R text files, the first line (column headers) must have one item less than the subsequent ones (i.e. the top-left cell is empty). Values must be tab-separated. A # at the beginning of a line is a comment, and the whole line will be ignored when reading the file.

Miscellaneous Options

Indicate here the methods and options by which Rcrust will calculate compositions of stable phases

Options

Calculation choice {calcchoice}	String	"run.meemum" "newcalc" Default = newcalc
The method by which Rcrust will calculate the composition of stable phases. Run.meemum uses functions run.meemum and read.meemum to call Perple_X files outside of the R console. Newcalc loads these files into the R console during initialization. This allows the compositions to be calculated by calls within the R console (faster and less processing intensive).		
Perple_X build file {build.file}	String	
The name of the build file (the one generated by build.exe in normal perple_x use, but you can create one manually). P—T settings, axis, bulk compositions, etc found in this file will be ignored and replaced by the values defined by Rcrust. By default this is "meemum_build.dat"		
Meemum order PT {meemum.order}	Radio button selection	"TP" "PT" Default = TP
The order in which meemum expects P and T values to be specified. This varies from version to version (and perhaps also according to settings in the build or the option file), so it's probably wise to		

check what happens on your system, for this specific build file, by test-running meemum and watching the order in which it expects variables.

Melt model (melt name) {melt.name}	String	
The name of the melt model to use. It's probably going to be "melt(HP)" most of the time, but who knows, you may want to try something else...		

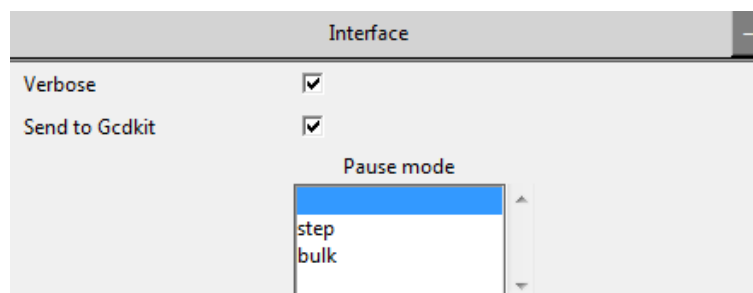
Solution models {use_sol_models}	Character vector (comma separated strings)	
The names of solution models to use. By default these come from the solution_file defined in init_meem.r (solution_model.dat). To view the available solution models in this file type "solution_models" into the R console and press [enter].		

Miscellaneous data {meemum_misc}	Character vector {comma separated}	
List of the thermodynamics properties that meemum outputs. You need to know them in advance. This may change with future versions of meemum. Note these are case sensitive. e.g. wt%, vol%, mol%, N(g), H(J), S(J/K), V(J/bar), Cp(J/K), Alpha(1/K), Beta(1/bar), Cp/Cv, Density(kg/m ³)		

Interface

Options for interacting with the program, doing the execution.

In any case it is wise to deactivate "buffered output" (in R gui for windows), at Miscbuffered output: this will allow the user to see things happening (otherwise the program will run silently, and print all the output the end – not very useful).



Options

Verbose {verbose}	Boolean	T (TRUE) F (FALSE)
Print lots of info on screen. Otherwise the info is kept at a minimum (warnings and some tracking information). Useful to see what is going on, obviously.		

Send to Gcdkit {to.gcd}	Boolean	T (TRUE) F (FALSE)
If true, the output file (defined by the output parameters) will automatically be loaded to GCDkit at the end of calculations. Requires GCDkit to be loaded first.		

Pause mode {pause}	List selection	"" "step" "bulk"
If "step" or "bulk", the code will pause after processing each step (or bulk) and wait for the user to press a key, therefore allowing to inspect the work being done (obviously more useful with verbose=T).		

Perplex options set in init_meem.r

Thermodynamic database file {thermo_file}	Character vector	Default = hp04ver.dat
The name of the thermodynamic data file to be used.		

Solution model file {solution_file}	Character vector	Default = solution_model.dat
The name of the solution model file to be used. To view the available solution models in this file type "solution_models" into the R console and press [enter].		

Perple_X option file {comp_file}	Character vector	Default = perple_x_option.dat
The name of the Perple_X option file to be used.		

Number of chemical components {number_components}	Integer	Default = 15
The number of chemical components to build the major elements from.		

Unit for bulk composition definition	Integer	0 = molar % 1 = weight % Default = 1
The unit proportion to use for bulk composition definition.		

Advanced user options (accessible through meemum_model.r)

Retention mode {retention_mode}	Boolean	T (TRUE) F (FALSE)
Allows phase extraction of melt to occur in a proportion such that it leaves behind a melt retention amount		

Retention unit {retention_unit}	Character vector	wt%, vol%, mol%
Units to use when defining the melt retention amount		

Calculation mode {calc_mode}	Character vector	normal poss = possibility matrix Default = normal
-------------------------------------	------------------	---------------------------------------------------------

Advanced setting toggling the calculation mode. Used to enter possibility matrix calculations.

PT definition {PT_def}	Character vector	file = defined through PT file build = from Rcrust GUI Default = build
Advanced setting toggling the PT definition mode. Used to allow PT definition from file.		

Unique bulks for each step {bulks_for_steps}	Boolean	T (TRUE) F (FALSE) Default = FALSE
Advanced setting toggling the use of unique bulks for each step.		

Alter bulk composition {alter_bulk}	Boolean	T (TRUE) F (FALSE) Default = FALSE
Advanced setting allowing the manual altering of the bulk composition.		

Step dependence {steps_are_independent}	Boolean	T (TRUE) F (FALSE) Default = FALSE
Allows steps to be treated as independent (bulk composition is no longer passed between steps but rather initial composition for each bulk or step is used for each step).		

Bulk dependence {bulks_are_independent}	Boolean	T (TRUE) F (FALSE) Default = TRUE
Allows bulks to be treated as dependent (this loops the parsing of bulk compositional change from one bulk to the other).		

Delta extraction mode {extr_delta_mode}	Boolean	T (TRUE) F (FALSE) Default = FALSE
Allows the calculation of deltas (positive gain in proportion of a phase between steps) for phase extraction		

Reaction buffering {reaction_buffering}	Boolean	T (TRUE) F (FALSE) Default = FALSE
Allows reaction buffering (threshold buffering) whereby phase extractions set on conditions are postponed by the number of reaction buffer steps to ensure continued exceedance of the threshold.		

Useful functions in the R Console

`ls()` List all objects in the current environment

`Q()` Quits

`[Ctrl]+[w]` Toggles buffering of outputs

`Rcrust()` Manually launches the Rcrust GUI

Rcrust variables

PT [bulk] [step] \$ press \$ temp	list
List of pressure and temperature conditions for each step in each bulk	
crust [bulk] [step] [phase, detail]	list
The full system (FS). Contains details of the reactive subsystem (RS) at each step along with cumulative extract (ES) and addition (AS) subsystems. Phases in crust are reported as cumulative weighted averages.	
extract [bulk] [step] [phase, detail]	list
The extract subsystem (ES). Contains details of individual extracts including the extracted phase name, composition and proportion. Phases reported in extract are non-cumulative and only represent the individual phases extracted at each step.	
ph_add_data [bulk] [step] [phase, detail]	list
The addition subsystem (AS). Contains details of individual extracts. The extracted phase name, composition, proportion and additional properties	
c0 [detail]	vector
Bulk composition passed between points	
workingfile	Character vector
The current Working File	
work_dir	Character vector
The current Working Directory. This is the location of the folder containing the Working File	

Development

Developers of new features should know a few things on the structure of the code. When developing custom functions please stick to these conventions.

The following files are required; they must all be in the same directory (these are contained within the Rcrust folder which should simply be copied to the desired location):

- 1) From **Perple_X** suite:
 - a. The program *meemum.exe*
 - b. The various datafiles you wish to use, normally defined in the “build” file: thermodynamic datafiles, typically *hp04ver.dat* and *solution_model.dat* as well as the Perple_X option file, *perplex_option.dat*.
 - c. The rest of *perple_x* (*vertex*, *build*, *werami*, etc) are not required.

- 2) From **Rcrust**:
 - a. *Build.r*, this builds the Rcrust Graphical User Interface (GUI)
 - b. *meemum_model.r*, this houses the main calls to run Rcrust
 - c. Various *init_XXX* files, used to transform user input in data structures that Rcrust can understand.
 - i. *init_data_str.r* builds empty data structures (mostly lists, in R language)
 - ii. *init_bulk.r* sets the bulk composition(s) of the system
 - iii. *init_PT.r* sets the PT conditions for each step/bulk combination
 - iv. *init_kd.r* reads the partition coefficient data file
 - v. *init_ph_add.r* sets the phases to add
 - vi. *init_ph_extr.r* sets the phases to extract
 - vii. *init_mem.r* writes user inputs into a meemum build file
 - d. *main.r*, the core of the program, actually containing the functions and routines that do the real job.

Technically, each function works on a table called “thecomp”, that has the various phases (s.l., also including things like system, total extract, etc.) as rows and their properties (mostly composition, but since *perple_x* generates thermodynamic properties we keep them throughout the calculation) as columns. *Main.r* loops through each step and bulk, calculates and modifies thecomp, and eventually stores the final product in a list called *crust*, whose structure is `crust[[bulk]][[step]]`. So, for instance the SiO₂ content in the melt of bulk=4 at step=2 is `crust[[4]][[2]][“melt(HP)”, “SiO2”]` (assuming you use *melt(HP)* of course).
 - e. *meemum_connect.r*, a file containing functions used to call meemum from within R.
 - f. *newcalc* a file containing functions used to operate meemum within R.
 - g. *output.r*, an accessory routine that formats the output list into a more human readable table, and writes it to disk.
 - h. *Speedtest.r* a routine for checking the minimization speed
 - i. Various *xxx.dll* files which contain compiled libraries needed to perform calculations within R

Troubleshooting

A list of known errors that are unavoidable or are still to be fixed.

Bulk_ss system properties

Warning: some bulk system properties are reported as molar properties but perplex considers the bulk system to be one mol thus all molar properties need to be adjusted accordingly

Molar phase proportions

Only weight definitions of bulk and phases is currently possible, read.meemum cannot read molar phase proportions. If molar proportions for bulk are entered then bulk is molar but individual phases are weights thus phase extractions crash.

End of Run

On completing the run in R console when prompted to select outputs if anything is typed into the console and then [enter] is pressed the R console crashes.

Solution: Press [enter] before typing anything to re-activate the console

Silent Run

The R console by default returns a buffered output which forces the run to only display after the calculation is completed. To disable the buffering and view run data live deselect from R toolbar Misc/Buffered Output (for more run info activate verbose from [Interface](#)).

Scroll bar

The Rcrust GUI does not have a scrollbar as this feature is not yet supported by tcl/tk, to access buttons off of screen minimize some tabs.